THE DESIGN AND APPLICATIONS OF A TRANSIENT VISUALIZER

A Thesis

Presented to

The Faculty of Graduate Studies

and Research

The University of Manitoba

In Partial Fulfillment

of the Requirements for the Degree

Master of Science

in

Electrical Engineering

---

by

Leonard Edward Petrie

May 1959

ABSTRACT

The design of a transient visualizer is described in Part A. The instrument applies repetitive pulses to a network and the transient current or voltage can be visualized on the screen of an oscilloscope. The design of the thyratron control circuit is original with the author. Part B consists of the utilization of the instrument in the electric power field. The voltage distributions in a transformer and a three-phase induction motor winding are investigated. Also the visualizer is used in designing a potential divider and in determining the response of a magnetic amplifier.

TABLE OF CONTENTS

CHAPTER PAGE

LIST OF FIGURES

FIGURE PAGE

PART A

PART B

LIST OF TABLES

PREFACE

When an electric circuit changes from one steady-state of operation to another, it passes through a transition period in which the currents and voltages are not recurring periodic functions of time. During this period some of the most complex operating problems are encountered in the circuit.

The transient visualizer permits the visual display of a transient voltage or current. The visualizer applies repetitive pulses with a specific wave shape to a network and the transient current or voltage at any desired point may be displayed on the screen of an oscilloscope.

This thesis is divided into two major sections. Part A consists of the design of the transient visualizer. This includes the design of the thyratron charging and discharging circuits and the trigger circuit controlling this operation. Both an external trigger and beam trigger output are available for controlling the sweep of an oscilloscope. For the measurement of peak voltages, a peak-reading voltmeter is installed in the apparatus.

Part B consists of the utilization of the transient visualizer. The visualizer displays on an oscilloscope a transient current resulting from a capacitor discharge. To determine the accuracy of the equipment the transient current is calculated and the two results are compared graphically. The voltage distributions in a transformer winding and a three-phase induction motor winding are investigated. Then the visualizer is used in designing a potential divider and in determining the response of a magnetic amplifier.

The author wishes to express his sincere thanks to Professor J. P. C. McMath for his constant interest, and stimulating discussions, and to Professor R. A. Johnson for his invaluable suggestions during the preparation of this thesis.

The assistance of the National Research Council of Canada in providing funds for the development of this project is gratefully acknowledged.

PART A

DESIGN OF TRANSIENT VISUALIZER

CHAPTER I

INTRODUCTION

The first transient visualizer was developed by N. Rohats (Roh 1)* in 1936, and was called an "Oscillograph Electric Transient Analyzer". Rohats used a rectifier to charge a storage capacitor and a thyratron to discharge the capacitor as shown in Fig. I-1.

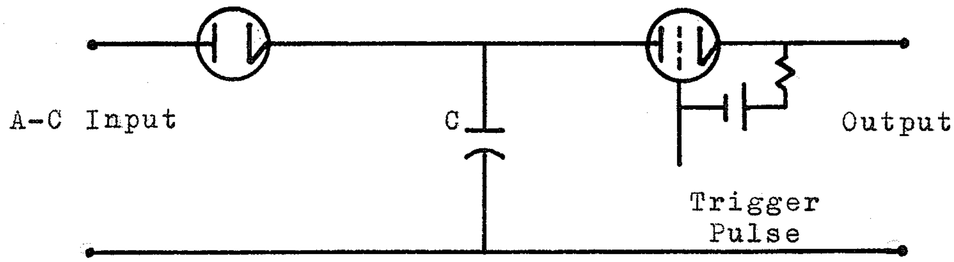

Fig. I-1 Rectifier and Thyratron Control Circuit

The capacitor C was charged positively during the first quarter-cycle of the supply voltage as shown in Fig. I-2.

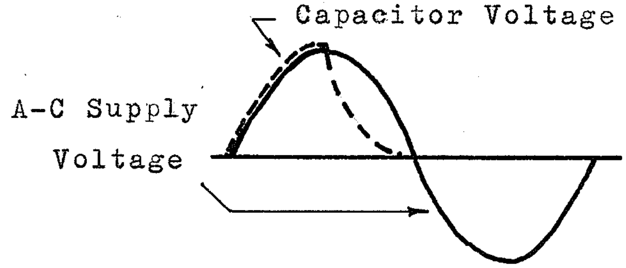

Fig. I-2 Capacitor Voltage Waveform

After a quarter-cycle, the inverse voltage was greater than the forward voltage and the rectifier isolated the capacitor from the supply voltage. The thyratron was biased

*Notation in parenthesis refers to the Bibliography sufficiently negative so that it could not conduct unless a large positive pulse was applied to the grid. After a quarter-cycle, the grid was triggered and the capacitor discharged into the external circuit. The above charging and discharging action repeated itself every cycle.

In Rohats' apparatus, no provision was made to examine transients longer than three quarters of a cycle. If longer transients occurred, the thyratron and rectifier would be conducting simultaneously and the supply voltage would be applied directly across the output.

Another disadvantage of the earlier transient visualizers was their low output power. This was due to the low current and voltage ratings of the rectifiers and thyratrons available at that time. Since then, more modern tubes with higher ratings have become available.

In the circuit designed by Rohats the sweep of the oscilloscope was triggered a fixed time before the thyratron was allowed to conduct. This thyratron trigger delay was necessary because of the inherent delay in the sweep circuit of an oscilloscope. Also, if no delay was provided irregularities present at the start of the sweep would cause a nonuniform movement of the electron beam. A bright spot would occur on the screen and obscure the leading edge of any waveform close to the start of the trace.

The oscilloscopes available to the author had this undesirable delay and distortion in the sweep. In order that the transient waveform could be displaced from the start of the trace for all sweep speeds, a variable delay was incorporated in the instrument.

In the design of the transient visualizer the disadvantages mentioned above were reduced and in some cases eliminated completely.

CHAPTER II

THYRATRON CONTROL CIRCUIT

With the visualizer developed by Rohats, a transient period longer than three quarters of a cycle (.012 seconds if 60 cycle supply) could not be observed. In this newly developed visualizer the transient period is extended to 1.8 seconds. This is accomplished by using two grid-controlled thyratrons as shown in Fig. II-1.

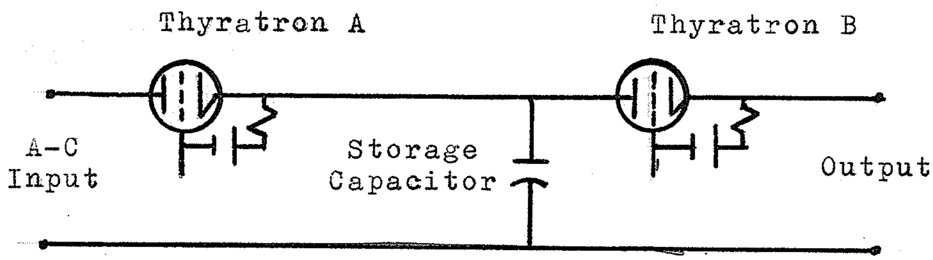

Fig. II-1 Thyratron Control Circuit

Both thyratrons are biased sufficiently negative so that conduction cannot commence until a positive pulse is applied to the grid. Thyratron A is triggered at the start of the sinusoidal wave. After a quarter cycle, the inverse voltage is greater than the forward voltage and conduction ceases. Then, thyratron B is triggered and the capacitor discharges into the wave shaping circuit. The conduction time of the discharge thyratron depends on the length of the transient. Therefore, by controlling the time between the discharging and charging operation very long transients can be observed. The above statements can be illustrated by the following diagram, Fig. II-2, page 4.

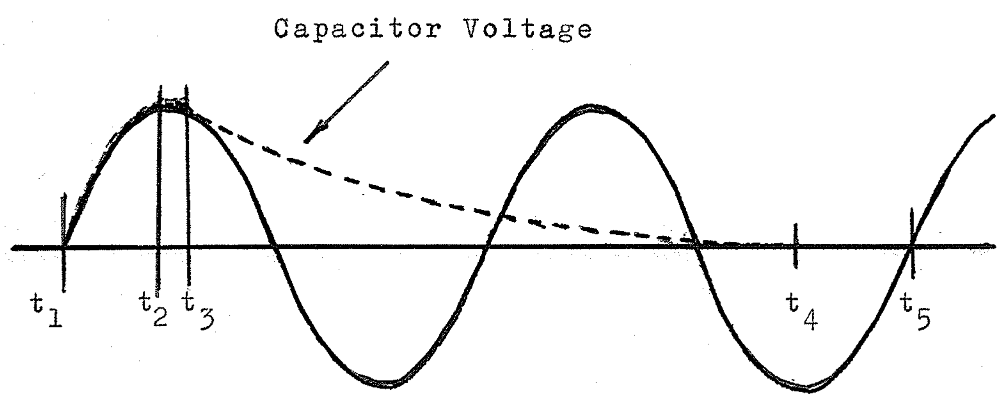

Fig. II-2 Waveform of Charging and Discharging Action

At t_1 thyratron A starts conducting
At t_2 thyratron A stops conducting
At t_3 thyratron B starts conducting
At t_4 thyratron B stops conducting
At t_5 above operation is repeated

Using the trigger circuit discussed in Chapter III the repetition rate of the instrument can be varied from 60 to .8 displays per second.

II - 1 ENERGY STORAGE

Three banks of oil capacitors are installed in the apparatus. By means of link connections an individual bank or any group of banks may be used for charging purposes. The capacitances available in various link positions with their maximum allowable voltage ratings are listed below.

TABLE II - 1 AVAILABLE CAPACITOR BANKS

Position	Max Voltage volts	Cap. uf
1	1,000	35
2	2,500	10
3	10,000	.5

The energy for the transient visualizer is obtained from an ordinary 60 cycle supply source and increased to a higher voltage by means of a transformer. The current flowing through the transformer and charging thyratron is shown in Fig. II-3.

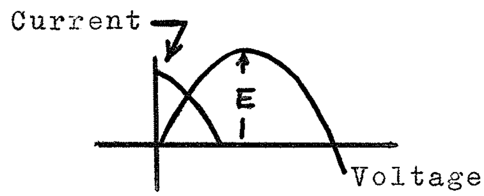

Fig. II-3 Transformer Current

Neglecting transformer impedance and tube drop the peak current flowing through the charging circuit is given by I_M = EwC amps.

where E = peak voltage in volts

w = $2\pi f$ = 377 @ 60 cycles

C = capacitance in farads

The peak currents based on the maximum allowable voltage ratings of the capacitor banks are listed in Table II-2.

TABLE II - 2 PEAK CURRENTS

Cap. uf	Max Peak Voltage volts	Peak Currents amps.
35	1,000	13.2
10	2,500	9.2
.5	10,000	1.8

The most severe average and rms currents will occur at the most rapid repetition rate of the instrument. Thus at 60 displays per sec.,

$$I_{av} = \frac{I_M}{2\pi} \quad \text{and} \quad I_{rms} = \frac{I_M}{2\sqrt{2}}$$

In Table II-3 the maximum average and rms currents are listed for the three capacitor banks for a repetition rate of 60 displays per second.

TABLE II - 3 MAX. AVERAGE AND RMS CURRENTS

Cap. uf	I_{av} amps.	I_{rms} amps.
35	2.1	4.7
10	1.5	3.3
.5	.3	.6

Considering the rms currents in Table II-3, a low voltage charging transformer was installed in the apparatus with the following specifications.

Max. Primary voltage - 135 volts

Secondary voltage - 810 volts

Max. continuous Secondary current - 1.23 amps.

Max. continuous KVA rating - 1KVA

Noting the rms currents in Table II-3, it appears that the capacity of the transformer is not sufficient for continuous operation on the 35 uf and 10 uf capacitor banks at 60 displays per sec. However, in actual practice the peak, average, and rms currents are considerably less than the calculated values due to inductance and resistance in the transformer and conducting leads. The visualizer has been operated continuously at a repetition rate of 60 displays per second without apparent damage to the transformer.

The input voltage to the transformer is controllable with a variac that is situated on the front panel of the visualizer. For a larger charging voltage, external input terminals are provided at the rear of the apparatus.

II-2 TUBE SELECTION

The maximum continuous current a tube can conduct without danger of overheating or reducing its life is called the average anode current. However, repeated high instantaneous currents may shorten life even if the average current rating is not exceeded. Therefore, tubes have maximum instantaneous current ratings for normal operation called the maximum peak current. The maximum fault current is the largest value of abnormal peak current of short duration (0.1 sec. maximum) that should pass through the tube under the most adverse conditions of service. It is not intended for use under normal operating conditions because it will seriously reduce or even terminate tube life.

The maximum peak inverse voltage is the largest instantaneous voltage that may be allowed to appear across the tube in the inverse direction without danger of reverse conduction. The maximum peak forward voltage is the maximum instantaneous anode voltage in the forward direction which a suitably controlled grid can prevent from firing the tube.

For the charging thyratron a 5563-A was selected. From RCA Bulletin 5563-A-6-54 the maximum ratings were obtained.

Anode Current:

- Average - 1.8 amps.
- Peak - 10 amps.
- Fault - 50 amps.

Peak Anode Voltage:

- Forward - 20,000 volts
- Inverse - 20,000 volts

The peak inverse voltage on the thyratron is approximately twice the peak charging voltage for long transient periods as shown in Fig. II-4, on page 8.

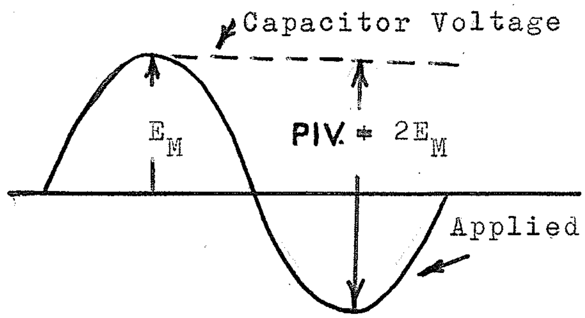

Fig. II-4 Peak Inverse Voltage

Therefore, the maximum allowable charging voltage is

$$V_c = \frac{20,000}{2\sqrt{2}} = 7070 \text{ volts r.m.s.}$$

From Tables II-2 page 5 and II-3 page 6, the maximum peak current is 13.2 amps. and for a repetition rate of 60 displays per second the maximum average or d-c current is 2.1 amps. The peak and average currents are in excess of the manufacturer's ratings. However, the charging thyratron has been used with the excess currents with no apparent damage.

For the discharging thyratron, a 5563-A was employed for high voltage output and a EL C16J for low voltage. From Electrons Incorporated Manual, "Rectifier and Control-Rectifier Tubes", the EL C16J has the following maximum ratings.

Peak Anode Voltage

Forward - 1,000 volts

Inverse - 1,250 volts

Anode Current

Average - 18 amps.

Peak - 100 amps.

Fault - 1,000 amps.

The EL C16J thyratron has been used for over 48 hours with no adverse effects with a peak anode current of 200 amps. lasting 5 usec., and a repetition rate of 60 displays per second. Since the inverse peak anode voltage is never greater than the forward voltage, a 1,000 volt, 200 amp. peak current output is available using the EL C16J thyratron.

Using the 5563 thyratron a 10 KV., 13.2 amp. peak current output is available. As discussed previously a peak current of 13.2 amps. was used with no apparent damage to the thyratron.

II-3 FILAMENT AND BIAS SUPPLY

All three thyratrons are provided with separate filament transformers. Since overheating the filament shortens tube life by evaporating the cathode, and insufficient heating damages the emissive surface by excessive ion bombardment, the primary of each transformer consists of a 110 volt winding with ± 3%, ± 6% taps. Since the thyratrons have a directly-heated cathode, the secondary winding of the filament transformers are insulated from ground as follows: 5563 - 30KV., EL C16J - 4KV.

From RCA Bulletin 5563-A-6-54, a bias of -60 volts prevents the unpredicted firing of the 5563 thyratron. Also, from Electrons Incorporated Manual "Rectifier and Control-Rectifier tubes", a bias of -150 volts prevents the unpredicted firing of the EL C16J thyratron. Since the bias supply has to be insulated for maximum cathode voltage to ground, a radio frequency oscillator supply was considered. Because of the difficulty in supplying a large power output from an oscillator it was decided that dry cell batteries mounted on bakelite insulation would be quite satisfactory. Since battery current flows only when the thyratron is conducting, the battery should last its shelf life. The following battery voltages are used to bias the thyratrons: 5563-A - 67½ volts, EL C16J - 157½ volts.

When the thyratron is triggered the grid is driven positive, and in order to limit the grid current a 1,000 ohm resistance was placed in series with the grid. To limit the grid current when the thyratron fires, the following grid to cathode resistances were used: 5563-A 10 kilohms, EL C16J - 33 kilohms. The above resistances maintain the grid currents below their maximum ratings after the thyratron fires. Also the resistances are smaller than the maximum allowable of 100 kilohms recommended by the manufacturers. If the maximum allowable resistance is exceeded the grid circuit tends to make the striking point less definite and the action of the valve less reliable. (Par 1)

The filament and bias circuits for the thyratrons are shown in Fig. II-5, page 12.

II-4 PLUG BOARD PANELS

The EL C16J thyratron provides a low voltage output and the 5563-A thyratron a high voltage output. By means of a plug board and panel shown in Fig. II-6, page 13, it is possible to switch from high to low voltage operation or vice versa. The panel consists of banana jacks (designated by circles) mounted on a bakelite panel and numbered 8, 9, 10, etc. These numbers correspond to those shown in Fig. II-5, page 12. The spacing between the jacks is greater than 2 inches in order to insure sufficient insulation at the maximum output voltage of 10KV.

The banana jacks 9, 12, and 15 are common connections for low or high voltage operation. Thus, a plug board can be used to connect jacks 8 -9, 11 - 12 and 14 - 15 for high voltage or jacks 9 - 10, 12 - 13, and 15 - 16 for low voltage operation. The plug board consists of banana plugs mounted on a bakelite panel and connected as shown in

Fig. II-6b.

Terminals are available on the panel for measurement of filament and bias voltages. For safety reasons all measuring terminals are inaccessible when the plug board is connected to the panel. The removal of the plug board disconnects the discharge circuit from the charging thyratron and storage capacitors. This provides protection against high voltages if bias and filament voltage measurements are performed when the charging voltage is applied to the circuit. In case the filament switch is accidently turned to the off-position during the actual operation of the visualizer, a plug link (connecting plugs 17 - 18, or 19 - 20) applies heater voltage.

Some means must be provided for discharging the storage capacitors when a capacitor bank is changed. A plug board and panel were designed to perform this operation. The removal of the plug board actuates a spring switch on the panel that discharges the capacitors to ground through a 10 ohm resistor. Due to the simplicity of the plug board, a diagram of it is not shown. On the panel shown in Fig. II-7, page 13, links are provided for the selection of an internal or external transformer. Normally, the link is connected to the internal position. Also, by means of link connections an individual bank of capacitors or any group may be used for charging purposes. Terminals are available for the measurement of filament and bias voltages and the plug board must be removed for these measurements.

Both the charging and discharging thyratron panels are mounted at the rear of the transient visualizer, At least 3" of bakelite insulation separates the banana plugs from the grounded frame. If procedure to the rear of the cabinet is necessary during the operation of the visualizer, always remove both plug boards and then make the necessary changes. If the above instruction is followed no harm can occur to individuals.

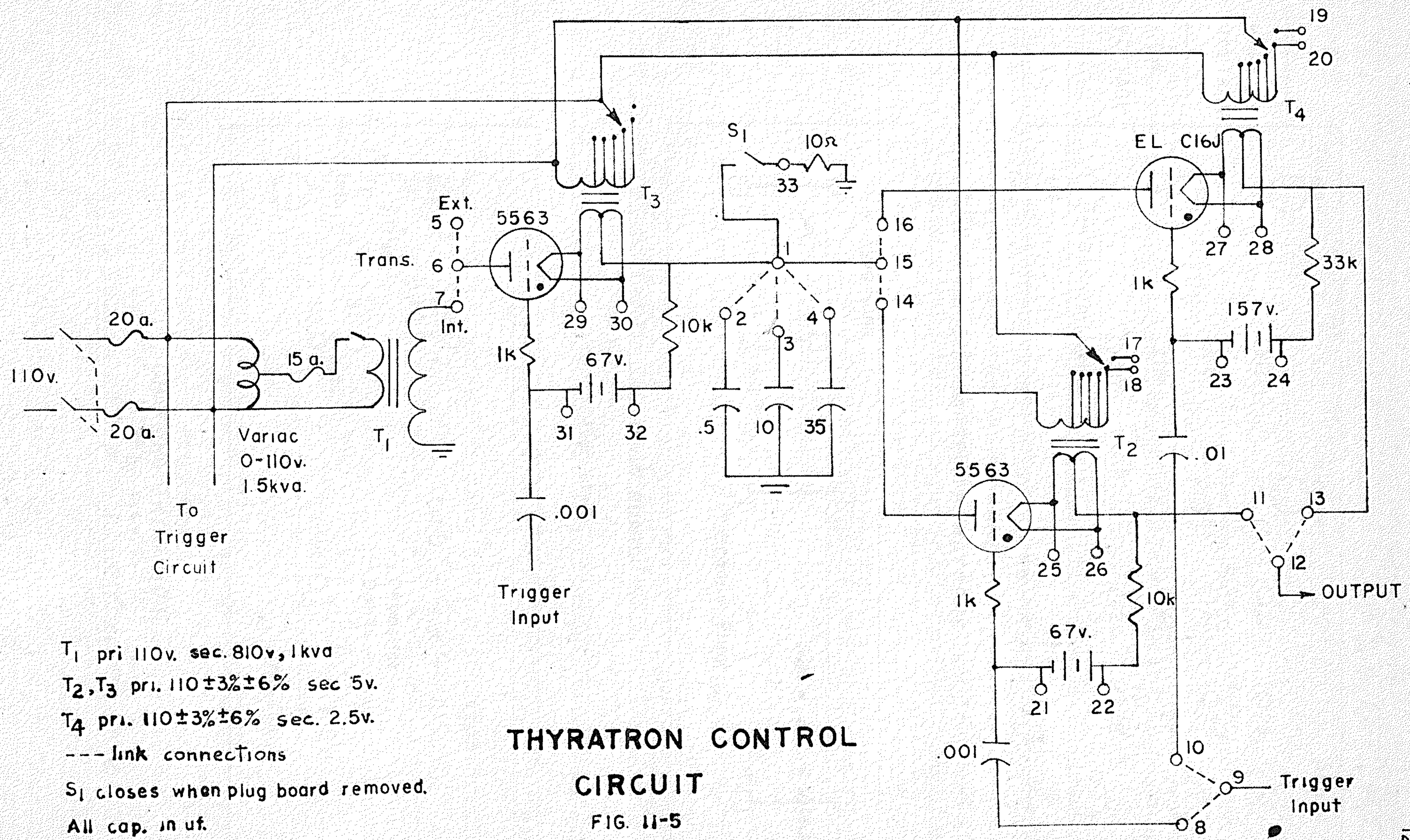

THYRATRON CONTROL CIRCUIT

FIG. 11-5

T_1 pri 110v. sec. 810v, 1kva

T_2, T_3 pri. 110±3%±6% sec 5v.

T_4 pri. 110±3%±6% sec. 2.5v.

--- link connections

S_1 closes when plug board removed.

All cap. in uf.

CHAPTER III

INTERNAL TRIGGER CIRCUIT

The pulse that triggers the charging thyratron must be synchronized with the 60 cycle supply voltage and occur at the beginning of the cycle. To accomplish this, the sine wave is converted to a square wave with the same period and phase as the supply voltage. Then the square wave is differentiated and the positive pulses fire the charging thyratron every cycle. However, a division circuit is needed to extend the firing time for the observation of long transients. A cathode-coupled monostable multivibrator is used as a divider. From the divider a portion of the output is used to trigger the charging thyratron. The discharge thyratron can conduct any time after a quarter cycle since conduction ceases in the charging thyratron. A delayed pulse from the divider is used for this purpose. The block diagram of the trigger circuit is shown in Fig. III-1, page 15.

III-1 THE CATHODE-COUPLED CLIPPER

Many types of circuits will convert a sine wave into a square wave. Various diode clipper circuits were designed and rejected because the discontinuities on the square wave were not sharp and definite.

The cathode coupled clipper was finally selected and it constitutes tubes V_{1a} and V_{1b} in Fig. III-2a, page 22. The output of V_{1a} consists of a sine wave with the negative portion clipped. Then, this is applied to V_{1b} and the positive half of the wave is clipped. The clipping levels can be adjusted by varying the bias on the two tubes. By properly choosing the value of bias for each tube the input wave is clipped symmetrically with respect to ground. Between the clipping levels the circuit is a linear amplifier

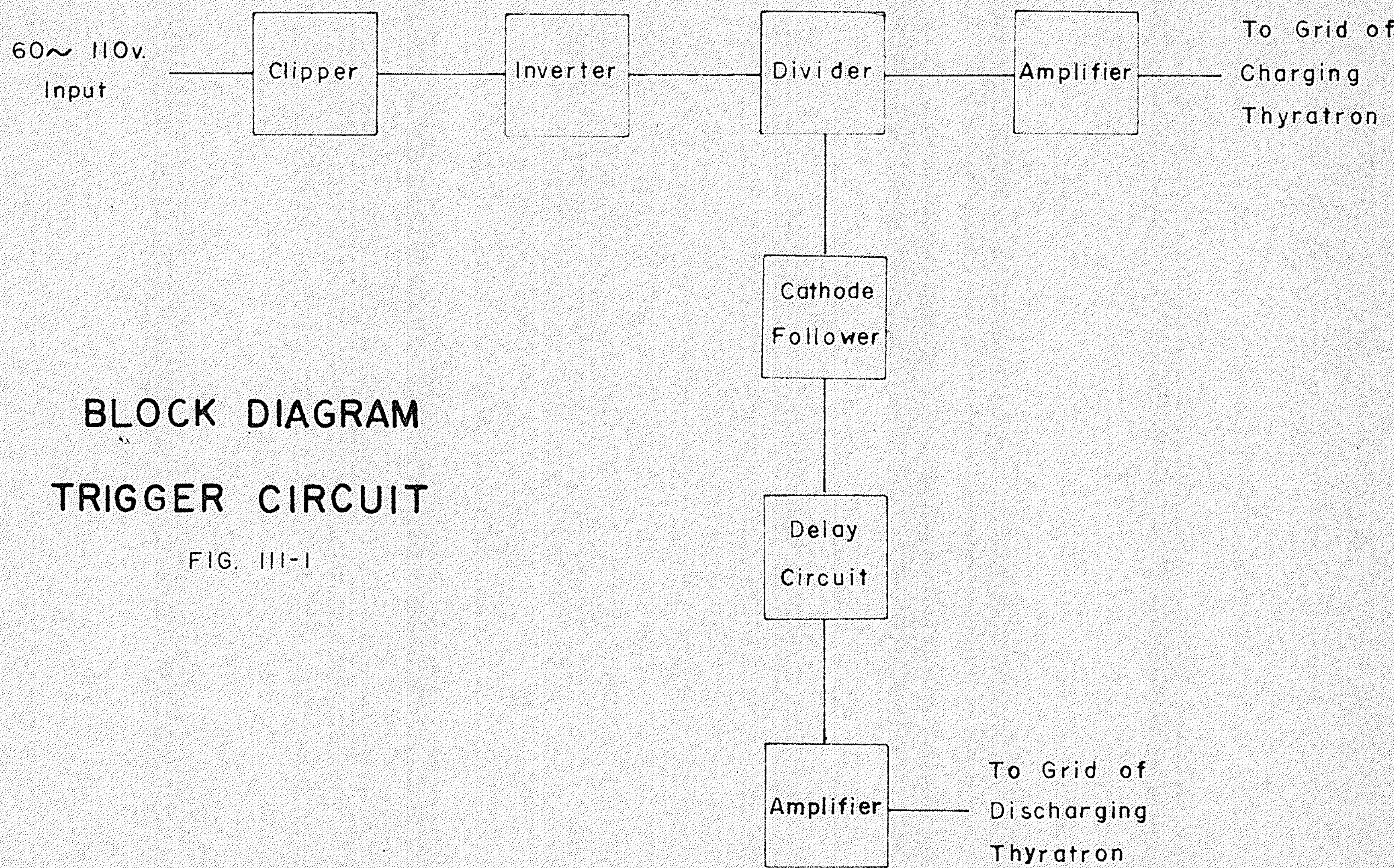

BLOCK DIAGRAM

TRIGGER CIRCUIT

FIG. III-1

without inversion. Since the cathode resistance is a large value, the line voltage (110 volts) can be applied directly to the input without drawing excessive grid current. Because of these features the circuit proves to be an excellent double-ended clipper. The output waveform is shown in Fig. III-3a, page 24.

The square wave is then differentiated and applied to an inverting amplifier (V_2). The 6C4 triode is biased so that the positive output pulse is clipped. The output wave from the amplifier is shown in Fig. III-3b, page 24.

III-2 THE CATHODE-COUPLED MULTIVIBRATOR

The output from V_2 (Fig. III-2a, page 22) is applied to a monostable multivibrator for division. Both the cathode-coupled and plate-coupled multivibrators were considered as division circuits. However, the cathode-coupled circuit consisting of V_{4a} and V_{4b} in Fig. III-2a was selected for the following reasons:

1. No negative supply is required.
2. The plate of V_{4b} is not in the regenerative loop and therefore an isolated output can be obtained.

The trigger arrangement shown in Fig. III-2a, page 22 using the diode V_{3a} is very advantageous. At the instant of transition the plate of V_{4a} drops, the diode no longer conducts, and the triggers are isolated from the multivibrator in the unstable state.

Consider the operation of the cathode-coupled multivibrator. In the stable state V_{4b} is conducting and the plate current flowing through the cathode resistor cuts off V_{4a}. A negative pulse applied to the plate of V_{4a} triggers the multivibrator to its unstable state in which V_{4a} is conducting and V_{4b} is nonconducting. The capacitor C charges through the resistance R until the potential at the grid of V_{4b} rises to the critical point where the triode V_{4b} conducts. A regenerative action restores the multivibrator to its stable state. The first trigger now applied will switch the multivibrator back to its unstable state. The plate resistance of V_{4a} is made large in order to reduce the dependence of the current upon the tube characteristics. The plate resistance of V_{4b} is kept small since the phase delay between the input and output trigger depends on the rate of rise of the output trigger.

In Appendix A an expression is derived for the period of the multivibrator. From equation A.6, page 71,

$$T = \frac{1}{w} \ln \frac{E_{bb}(A+1) - E_k}{E_{bb} - E_{co2} - \frac{AE_{bb}R_k}{R_1}} \qquad \text{III.1}$$

where $w = 1/(R + R_e)C$, $\quad A = R_1/\left[R_1 + r_p + (u+1)R_k\right]$

$R_e = A\left[r_p + (u+1)R_k\right]$

Comparing Figs. A-5 page 67 and III-2a page 22, the following equalities are obtained: $E_{bb} = 225$ volts, $R_1 = 100$k ohms, $R_k = 5$k ohms.

From the static plate characteristic for the 12AU7: $u = 16$, $r_p = 8$k ohms, $E_{co2} = 15$ volts.

Then, by calculation: $A = .52$, $R_e = 48.2$k ohms. The voltage E_k is calculated as indicated in equation A.1, page 69.

Therefore, $E_k = i_{b2}R_k = 15\text{x}5 = 75$ volts.

Then, $T = (R + 48.2\text{k})C \ln 1.305 = 2.66(R + 48.2\text{k})C$ seconds, where R and C are expressed in ohms and farads, respectively.

In Table III.1, page 18, the multivibrator period is calculated for various values of resistance and capacitance (measured to an accuracy of 2%). After the multivibrator is restored to its stable state, the first trigger pulse applied will switch it back to its unstable state.

TABLE III.1

THE MULTIVIBRATOR PERIOD

R ohms	C uf.	Period T sec.
275K	.01	.009
650K	.01	.018
1.3 meg.	.01	.035
5.4 meg.	.01	.145
1.5 meg.	.1	.40
2.6 meg.	.1	.69
3.5 meg.	.1	.93
6.7 meg.	.1	1.80

Since the monostable multivibrator is synchronized to the 60 cycle system, the calculated and also experimental pulse periods will be multiples of .016 sec. In Table III.2 the calculated pulse periods are compared with the experimental periods. The faster pulse periods (.016 - .40 sec.) were measured accurately with a cathode-ray oscilloscope. The slower pulse periods were measured with a brush oscilloscope to an accuracy of ± 2 cycles, i.e. .032 sec. At the slower periods a discrepancy exists between the calculated and experimental results. In the calculated pulse periods, errors are introduced using average plate static characteristic curves and nominal resistance values for R_1 and R_k.

TABLE III.2

COMPARISON OF THE CALCULATED AND EXPERIMENTAL PULSE PERIODS

Calculated Pulse Period seconds	Experimental Pulse Period seconds
.016	.016
.032	.032
.048	.048
.16	.16
.40	.40
.70	.69
.94	.95
1.80	1.85

Photographs of the grid and plate voltages, and the division action of the multivibrator are shown in

Fig. III-3c, page 25.

From the plate of V_{4a} Fig. III-2a, page 22, the pulse is differentiated and applied to the 807 power amplifier. Normally the tube is conducting heavily, and the negative pulse cuts off the tube causing a large positive pulse to appear at the plate. A d.c. power supply of 350 volts is required for an output pulse of 220 volts. This pulse is used to trigger the charging thyratron.

III-3 DELAY CIRCUIT

The voltage at the plate of V_{4b} Fig III-2a, page 22, is differentiated and applied to a cathode follower and diode clipper (V_6 and V_{3b}) Fig. III-2b, page 23, and then to a delay circuit. At first the screen coupled phantastron was considered for delay purposes, but it requires a negative supply voltage and the positive output pulse from the screen is loaded by the suppressor circuit.

Both of these faults are corrected in the cathode-coupled phantastron as shown in Fig. III-4. The main disadvantage of this circuit is the gain loss caused by cathode degeneration.

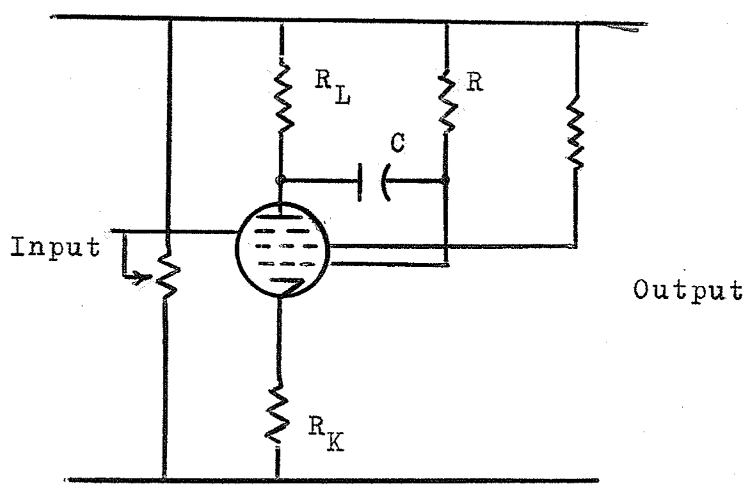

Fig. III-4 Cathode-Coupled Phantastron

Consider the operation of the cathode-coupled phantastron circuit. In the quiescent state, the suppressor to cathode voltage is negative and no plate current flows. If a sufficiently large positive pulse is applied to the suppressor, plate current flows and the plate voltage drops. This drop is transmitted to the grid and starts the well known Miller integrator action. The rate of fall of plate voltage is approximately linear and inversely proportional to the product RC. (Mar 1) When the anode bottoms, the grid potential increases causing the cathode voltage to rise above the suppressor voltage and plate current is again cut off. The plate rises exponentially to E_{bb} with the $R_L C$ time constant. A square wave output is produced across the screen resistance by the change in screen current. When the plate current begins to flow the screen current is reduced causing a vertical rise in screen voltage. When the anode bottoms a vertical drop occurs, thus forming the square wave.

By differentiating the screen voltage a negative pulse is obtained that is delayed a specific time from the input pulse.

The actual phantastron circuit (V_7 and V_8 in Fig. III-2b, page 23) is modified from the one discussed in Fig. III-4, page 19. The plate voltage is varied by means of a potentiometer and a diode V_7, and this varies the width of the screen waveform as shown in Fig. III-5, page 21. The variable delay is required so that the delay time (.004 sec.) can be readjusted when the pentode ages.

The output pulse from the phantastron is then differentiated and amplified. An 807 power amplifier is used and is identical to the one discussed previously. The output is used to trigger the grid of the discharge thyratron.

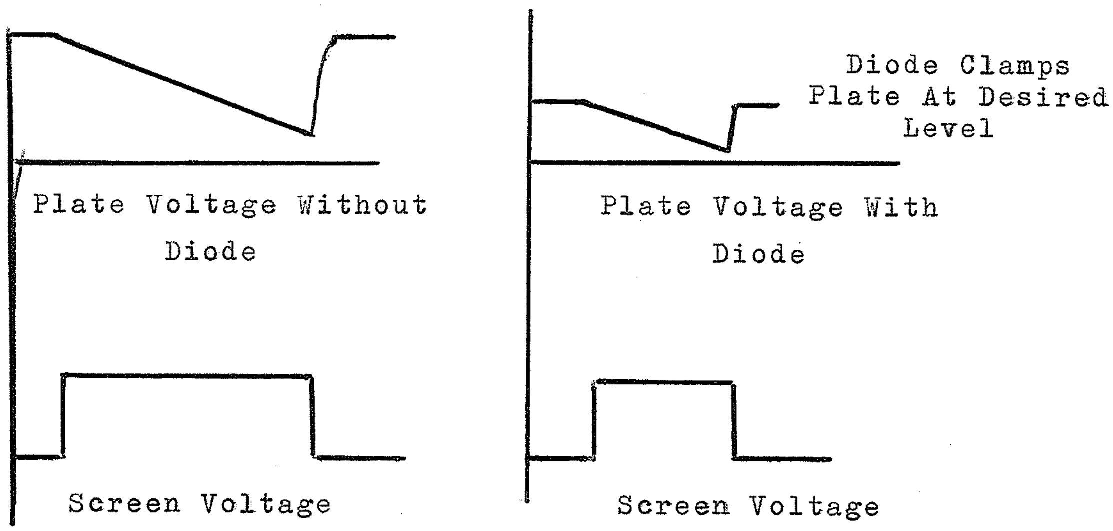

Fig. III-5 Variation of Pulse Width

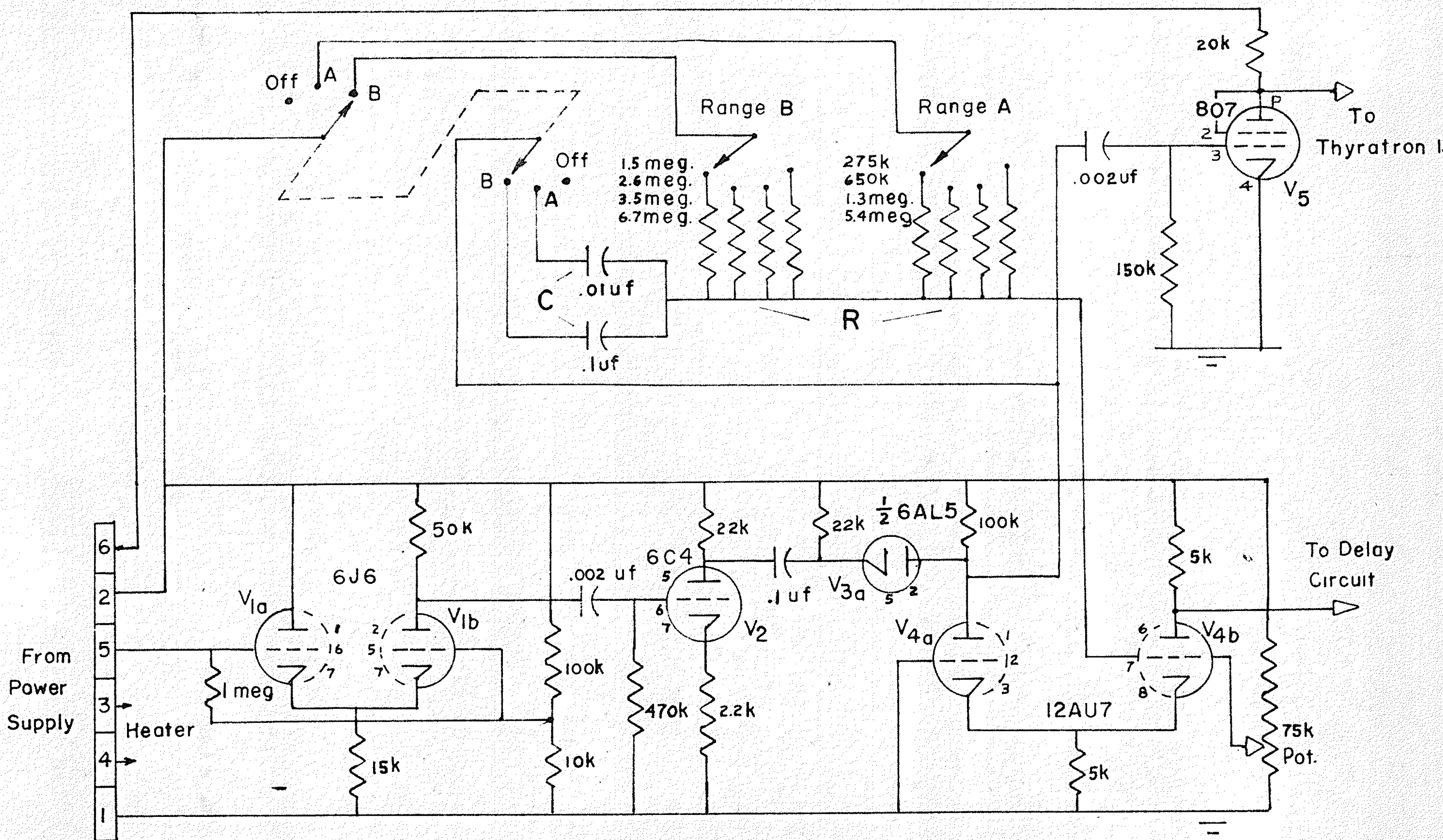

TRIGGER CIRCUIT

FIG. III-2a

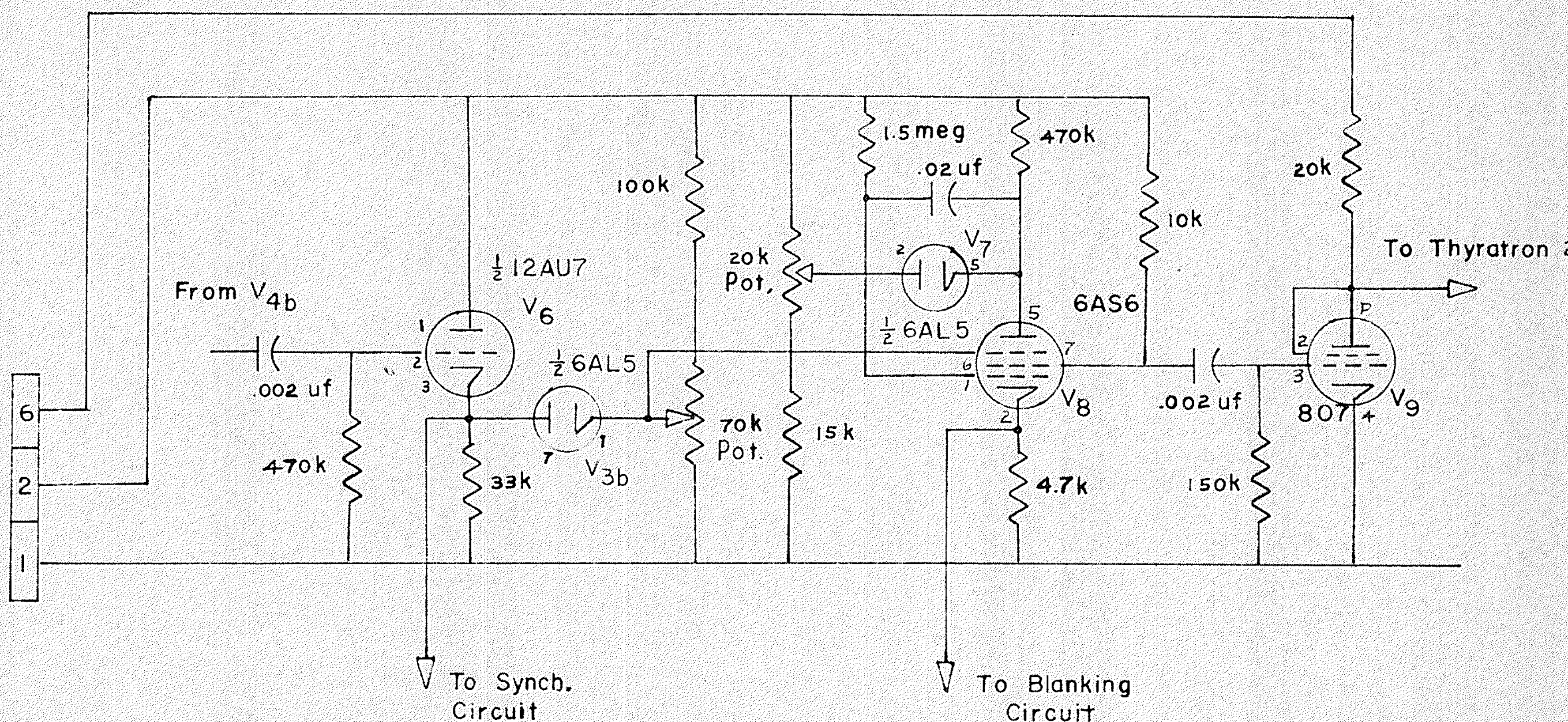

TRIGGER CIRCUIT

FIG. III-2b

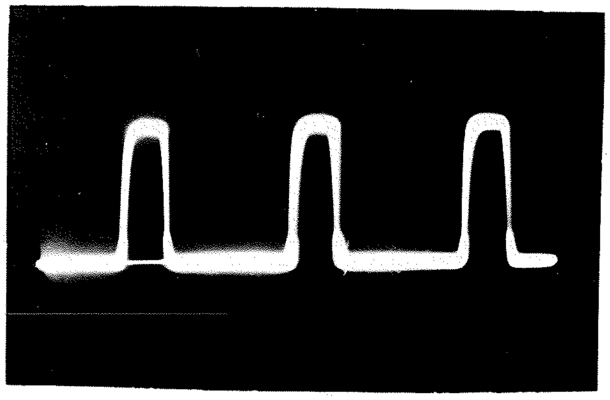

Clipper Output Wave

Fig. III-3a

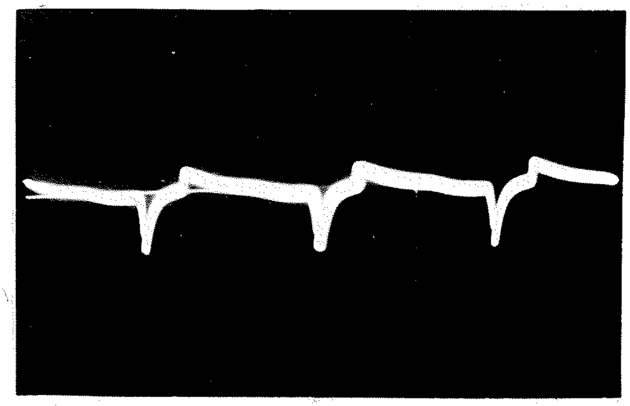

Divider Input Pulse

Fig. III-3b

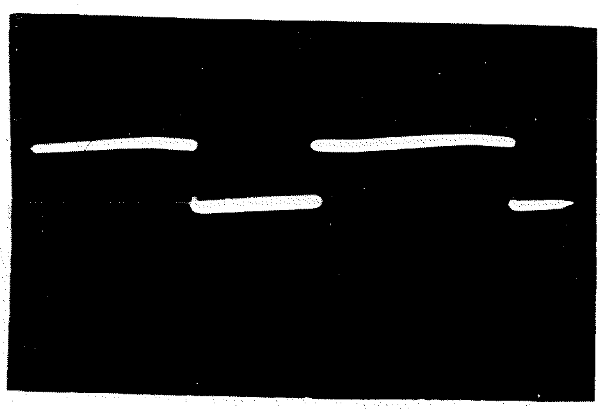

Waveform of Plate Voltage /5

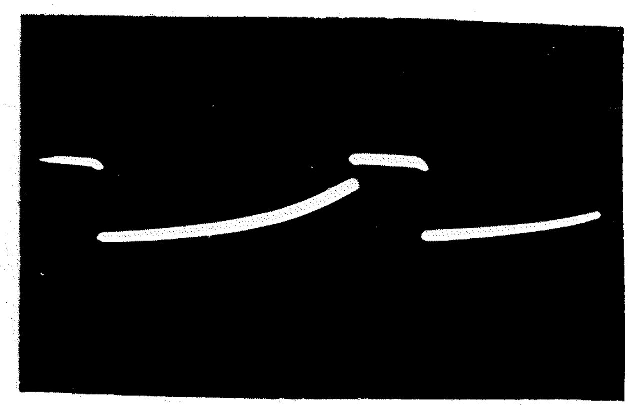

Waveform of Grid Voltage

Fig. III-3c

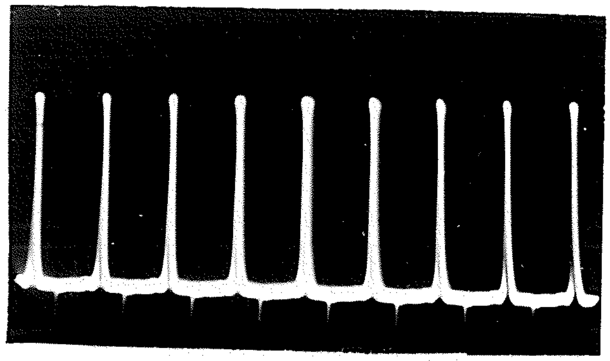

60 pps.

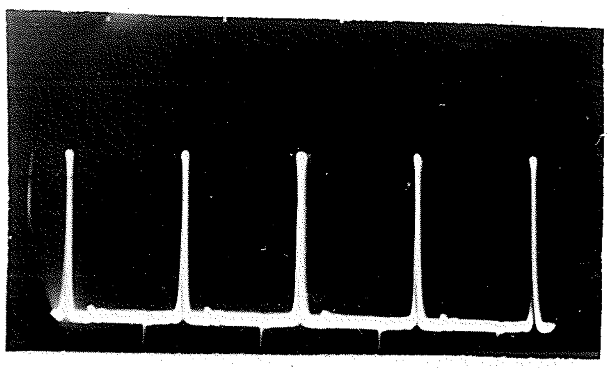

30 pps.

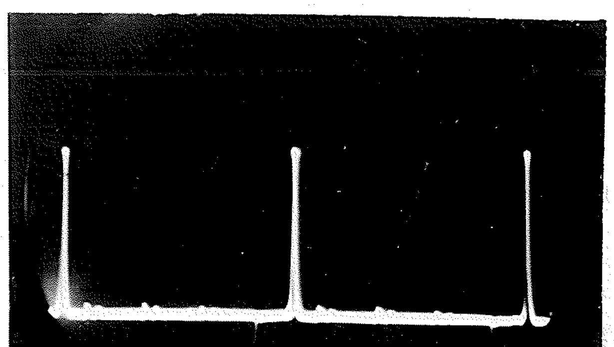

20 pps.

Division Action of Multivibrator

Fig. III-3c. continued
from previous page

CHAPTER IV

EXTERNAL TRIGGER CIRCUIT

An external synchronizing and a beam trigger output are available for controlling the sweep and beam brightness on Cossor oscilloscope 1049 MK II and 1049 MK III.

IV-1 EXTERNAL SYNCHRONIZING CIRCUIT

As discussed previously, it is very advantageous to have the sweep of the oscilloscope start before the transient wave arrives at the vertical deflection plates. The pulse that triggers the discharge thyratron is delayed one quarter of a cycle from the start of the 60 cycle sinusoidal wave. The transient wave observed on the oscilloscope will always occur after the discharge thyratron fires. Thus, the external synchronizing pulse can be delayed less than a quarter cycle from the start of the 60 cycle sinusoidal wave and the sweep will commence before the transient is initiated.

The synchronizing pulse reference is taken from the output of the cathode follower V_6 in Fig. III-2b, page 23. A variable delay is obtained from a phantastron circuit V_{10} in Fig. IV-1, page 29, that is identical in operation to the one discussed in Chapter III. The screen output is differentiated and brought out to terminals on the front panel. The sweep of the oscilloscope can be initiated zero to .004 seconds before the discharge thyratron conducts.

IV-2 BEAM TRIGGER

In the Cossor oscilloscope model 1049 MK II an electrical beam trigger control is available for switching the cathode-ray tube-beam. The tube trace is initially invisible and only restored to view by the application of an external negative DC signal of 12 volts or more to the "Beam Trigger" terminal. The trace remains visible as long as the voltage is applied.

In the Cossor oscilloscope model 1049 MK III the application of a negative DC signal causes the beam to be switched off or blanked, and thus, it is unsuitable for transient display purposes. However, a mechanical beam trigger control is available, which enables the beam to be switched on by applying a resistance of 8,000 ohms or more from "Intensity Mod." terminal to ground. A voltage of 60 volts positive is available at the terminal for a plate supply for a vacuum tube. However, the mechanical trigger is not suitable in the MK II model because it switches the tube-beam off.

Thus, two external beam trigger outputs were incorporated in the transient visualizer. One output operates the electrical beam trigger on the MK II oscilloscope and the other the mechanical beam trigger on the MK III.

The transient that is to be observed starts when the discharge thyratron conducts. During the transient period the beam should be switched on. Therefore, the start of the beam switching should occur when the thyratron fires and last as long as the transient.

This is accomplished by taking the pulse from the cathode of the phantastron that is instrumental in firing the discharge thyratron V_8, Fig. III-2b, page 23. This output is applied to a cathode follower V_{12} in Fig. IV-1, page 29, and then to a phantastron circuit identical to that above. The output is taken from the cathode of the phantastron and the pulse width can be varied from zero to .05 seconds by changing the potential at the plate as discussed previously. The pulse is 20 volts negative and can be used to switch the electrical beam trigger control in

Cossor Model 1049 MK II.

A triode V_{15} connected as shown in Fig. IV-1, page 29, operates the mechanical beam trigger control in the model 1049 MK III oscilloscope. In normal operation the tube is conducting heavily and the beam is off because the output resistance is less than 8,000 ohms. Now, the 20 volt negative pulse mentioned above can be applied to the grid of the triode driving the tube to cut-off. Since the output is open circuited the beam is switched on. The pulse width, which is variable from zero to .05 seconds, determines the time duration of the beam.

EXTERNAL TRIGGER CIRCUIT

FIG. IV-1

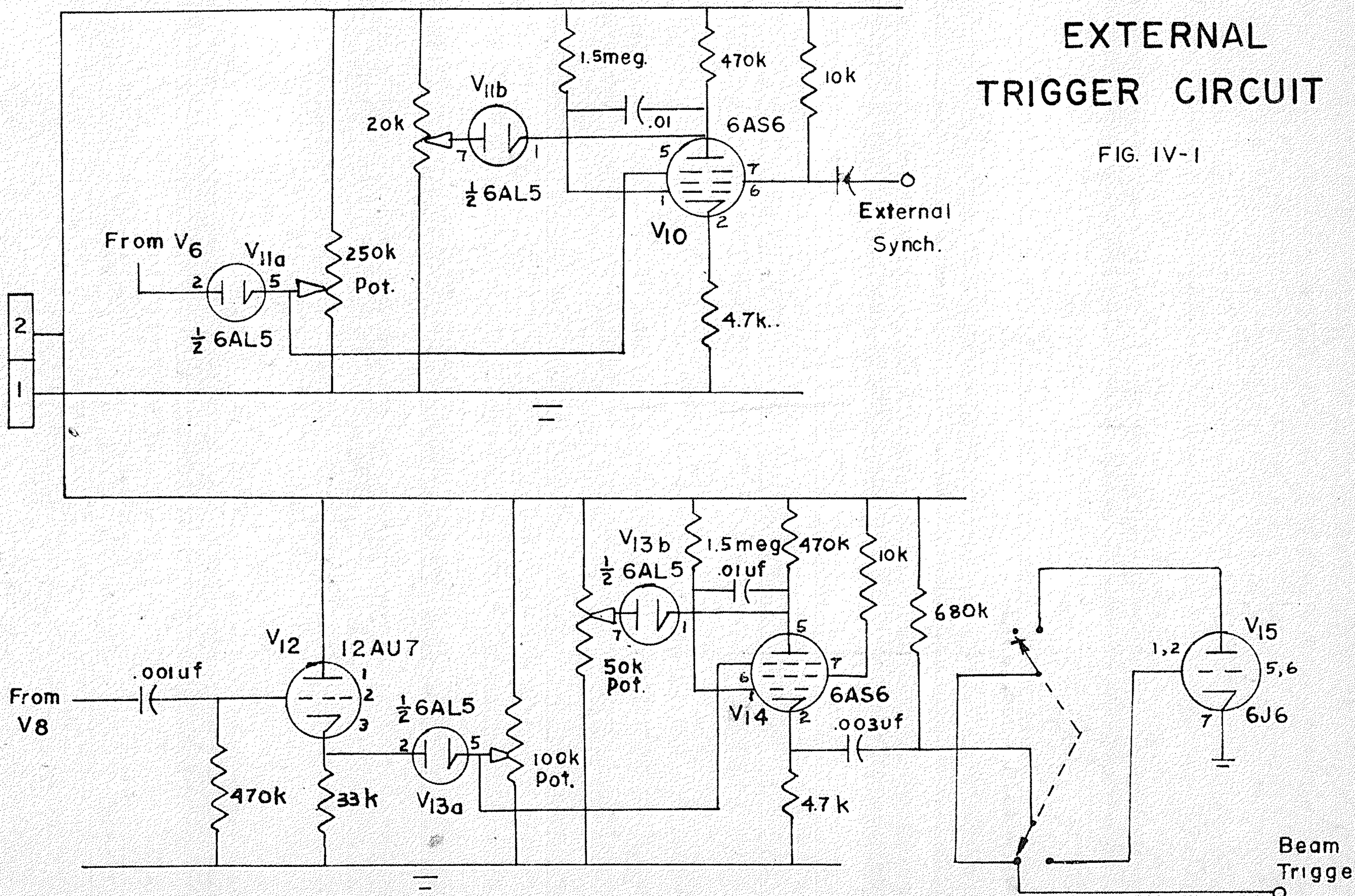

CHAPTER V

PEAK-READING VOLTMETER

V-1 THEORETICAL ANALYSIS

In order to facilitate the measurement of peak voltages, a peak-reading voltmeter was incorporated in the apparatus. The peak voltmeter circuit is shown in Fig. V-1.

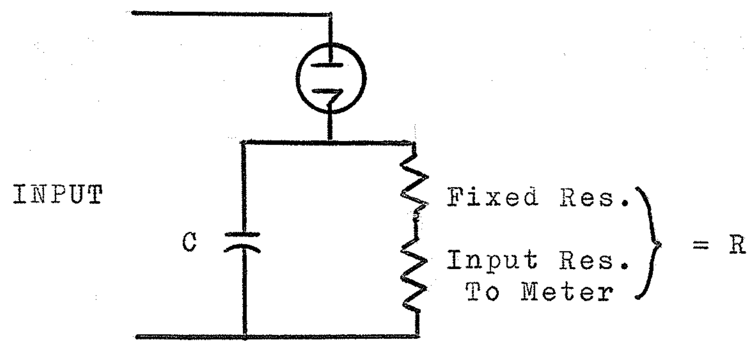

Fig. V-1 The Basic Peak Voltmeter Circuit

Where C = charging capacitor

R = fixed resistance plus input resistance of meter

An analysis of the circuit will determine the quality of the peak-reading voltmeter. When the diode conducts the above schematic diagram can be represented by the following equivalent circuit.

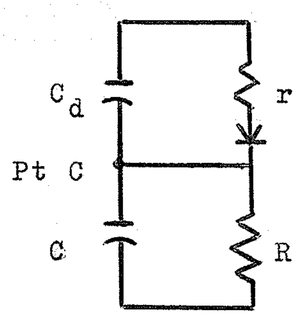

Fig. V-2 Equivalent Circuit of Peak Voltmeter where r = resistance of the diode

C_d = plate to cathode capacitance of the diode

Since the plate to cathode capacitance of the diode is small compared to the "charging" capacitor, it is neglected in the following analysis. Assume that the voltage waveform impressed on the voltmeter consists of regularly spaced rectangular-shaped pulses as shown in Fig. V-3. The potential at point C after a steady state has been reached is shown by the dotted line.

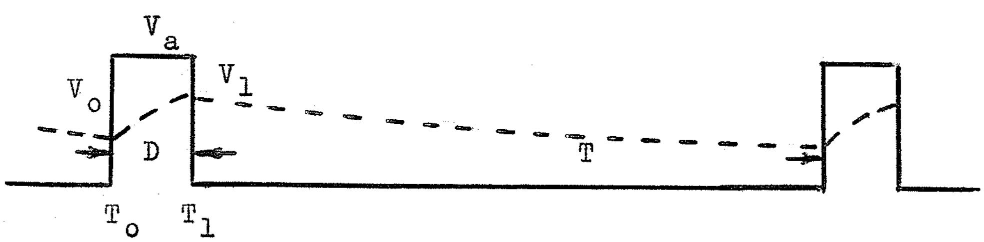

Fig. V-3 Potential on Capacitor C

where D = diode conducting time

T = time between successive pulses

V_a = actual maximum voltage

The potential at point C discharges to time T_o and then the diode commences to conduct. During conduction the capacitor voltage rises exponentially to V_1 with the rC time constant, while at the same time discharging through the resistance R. At time T_1, the inverse voltage is greater than the forward voltage and the diode ceases to conduct. After T_1 the capacitor discharges through R with the RC time constant and the cycle is repeated.

If the effect of the capacitance C discharging through the resistance R is negligible during the "charging time", (i.e. RC>>D) then from Fig. V-3 the following equations are obtained.

$$V_a - V_1 = (V_a - V_o)\,\epsilon^{-D/rC} \qquad \text{V.1}$$

$$\text{also } V_o = V_1\,\epsilon^{-T/RC} \qquad \text{V.2}$$

$$\text{Let } \epsilon^{-T/RC} = a \text{ and } \epsilon^{-D/rC} = b \qquad \text{V.3}$$

Solving equations V.1, V.2 and V.3 for V_o and V_1

$$V_o = \frac{V_a(1-b)}{\frac{1}{a} - b} \quad \text{and} \quad V_1 = \frac{V_a(1-b)}{1-ab}$$

If RC>>T and RC>>D, the average value of voltage is with negligible error $V_c = \frac{1}{2}(V_o+V_1)$. Therefore, the percentage error is given by

$$d = \frac{V_a - V_c}{V_a} = 1 - (1/2V_a)(V_o+V_1) \qquad \text{V.4}$$

Substituting values for V_o and V_1 in equation V.4

$$d = 1 - \frac{1}{2}\left[\frac{1-b}{\frac{1}{a} - b} + \frac{1-b}{1 - ab}\right]$$

which may be simplified to

$$d = \frac{1-a+b-ab}{2(1-ab)} = 1\Bigg/\frac{2(1-ab)}{1-a+b-ab}$$

$$= 1\Bigg/\left[1 + \frac{(1-b)(1+a)}{(1+b)(1-a)}\right]$$

Substituting values for 'a' and 'b' from equation V.3

$$d = 1\Bigg/\left[1 + \frac{(1-\epsilon^{-D/rC})(1+\epsilon^{-T/RC})}{(1+\epsilon^{-D/rC})(1-\epsilon^{-T/RC})}\right]$$

$$\text{and finally} \quad d = 1\Bigg/\left[1 + \frac{\tanh D/2rC}{\tanh T/2RC}\right] \qquad \text{V.5}$$

If rC>>D then equation V.5 can be simplified to

$$d = \frac{1}{1 + (DR/Tr)} \quad \text{provided RC>>T and RC>>D} \qquad \text{V.6}$$

V-2 DESIGN

For the peak-reading voltmeter the complete circuit diagram is shown below.

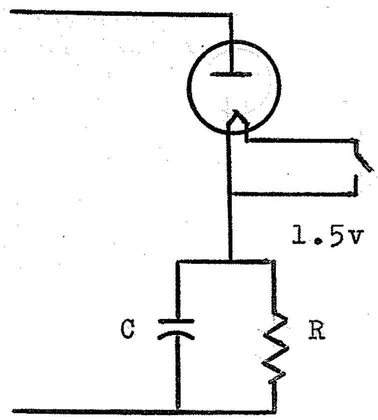

Fig. V-4 Complete Peak-Reading Voltmeter Circuit

Since the transient visualizer can produce a positive peak output voltage of 10KV., a diode was required with an inverse plate voltage rating greater than 10KV. The 1B3 GT diode was selected as the rectifier due to a peak inverse plate voltage rating of 30KV., and filament requirements of 1.25 volts, and 200 milliamps. Due to the cost and size of a filament transformer insulated for 10KV., a standard 1.5 volt flash light battery was used to heat the filament. In order that the filament is not on continuously a push button switch was inserted in series with the battery. The switch is normally in the off position and operates from an insulated bakelite rod that extends to the front panel of the visualizer. Due to its versatility, the Heathkit Model V7A V.T.V.M. was panel mounted and employed as the indicating instrument.

From equation V.6

$$d = \frac{1}{1 + (DR/Tr)}$$

provided $RC \gg T$, $RC \gg D$ and $rC \gg D$

In order that $RC \gg T$ and $RC \gg D$, the resistance R equals 1650 megohms and the capacitance C equals .075 uf. The resistance R consists of the following: a fixed resistance of 550 megohms, Heathkit Model 117 high voltage probe with 1090 megohms resistance, 10 megohm input resistance of meter.

For a filament voltage of 1.5 volts and a plate voltage of 50 volts, the plate current was measured as 33 milliamps. Thus, the diode resistance 'r' is approximately equal to 1500 ohms.

For short transients $T \gg D$, and with negligible error T can equal the period of the applied pulses. Now for a repetition rate of 60 displays per sec., calculate the smallest pulse width (D_m) that can be measured with an error of 3%. The error considered is that resulting from the impossibility of charging a capacitor completely to the applied voltage.

Therefore, $$D_m = Tr(\frac{1}{d} - 1)/R = .5 \text{ usec.}$$

Consider the restrictions on equation V.6

$RC = 123$ sec. and $T = .016$ sec. Therefore $RC \gg T$

$RC = 123$ sec. and $D = .5$ usec. Therefore $RC \gg D$

$rC = 75$ usec. and $D = .5$ usec. Therefore $rC \gg D$

Thus, the restrictions on equation V.6 are well satisfied.

For an error less than 3% the pulse width must be longer than .5 usec. for a repetition rate of 60 pulses per second. In the analysis it was assumed that a rectangular shaped wave was applied to the peak voltmeter. For a voltage wave with a sloping front, a larger pulse width is certainly required for an error less than 3%.

The peak voltmeter and a calibrated oscilloscope were used to measure the peak voltages of a 1.0 usec. and .5 usec. rectangular pulse. The peak voltmeter measured 3% low for the 1.0 usec. pulse and 6% low for the .5 usec. pulse.

CHAPTER VI

CALCULATION OF WAVE SHAPES

The basic impulse waveform used for testing the insulation of transformer and machine windings in Canada and the United States is the $1\frac{1}{2}$x40 microsecond wave. The figures in this designation indicate that the voltage rises to peak value in $1\frac{1}{2}$ microseconds and decays to half value in 40 microseconds. The $1\frac{1}{2}$x40 has been chosen as the standard because it can be obtained readily with the impulse generator and because it simulates the more severe lightning surges. However, the 1x5, 1x10, and the European standard 1x50 have been used extensively in testing insulation.

Now, consider a mathematical expression for the above wave shapes. The expression must be a reasonable approximation to the actual wave shape, and be handled without difficulty by standard mathematical treatment. Such an expression is

$$e = E(\epsilon^{-at} - \epsilon^{-bt}) \qquad \text{VI.1}$$

where E, a, and b are arbitrary constants.

Not only does equation VI.1 closely approximate the three shapes mentioned, but calculations based on it are relatively simple.

The simple exponential wave, is found by putting $b = \infty$, while 'a' is adjusted to give the desired length of tail. If $b = \infty$ and $a \to 0$, the wave approaches a unit step. In part B of the thesis, a unit step is approximated by such a wave.

In equation VI.1 the maximum voltage E_m occurs when

$$\frac{de}{dt} = 0$$

Therefore, the maximum voltage occurs at time T_m where

$$T_m = \frac{\ln b/a}{(b - a)a} = X/a \quad \text{where } X = \frac{\ln b/a}{b - a} \qquad \text{VI.2}$$

Then $$E_m = E(\epsilon^{-X} - \epsilon^{-Xb/a}) \qquad \text{VI.3}$$

The time T_h at which the wave decreases to half value is

$$E_m/2 = E(\epsilon^{-aT_h} - \epsilon^{-bT_h}) = E(\epsilon^{-XT_h/T_m} - \epsilon^{-XbT_h/aT_m}) \qquad \text{VI.4}$$

Substituting equation VI.3 in VI.4

$$\tfrac{1}{2}(\epsilon^{-X} - \epsilon^{-Xb/a}) = (\epsilon^{-XT_h/T_m} - \epsilon^{-bT_h/aT_m}) \qquad \text{VI.5}$$

From equation VI.2, aT_m is a function of b/a

From equation VI.5, T_h/T_m is a function of b/a

Bewley has plotted these functions (Bew 1) and from the graph the constants 'a' and 'b' in equation VI.1 can be found for any specified impulse wave.

It is now desirable to obtain a network that will produce the wave shape of equation VI.1. From Appendix B it is found that a simple series R, L, C network will produce the desired wave shape.

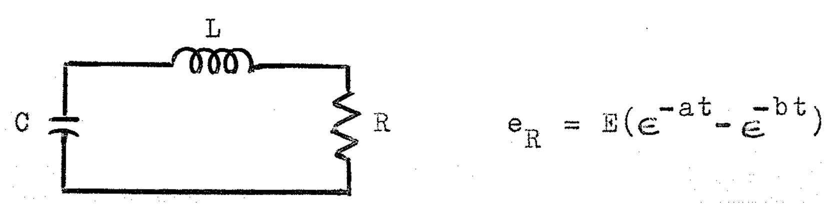

Fig. VI.1 Series R, L, C, Circuit

From Appendix B equations B.3 and B.4, page 74

$$L = 1/Cab \text{ henries} \qquad \text{VI.6}$$

$$R = \frac{a+b}{Cab} \text{ ohms} \qquad \text{VI.7}$$

if C is in farads.

Thus, for any wave $e = E(\epsilon^{-at} - \epsilon^{-bt})$, find 'b' and 'a' from Bewley's graph, and then calculate L and R in terms of C from equations VI.6 and VI.7.

In insulation testing the applied impulse wave is very short in duration. Thus, any resistance or inductance in the connecting leads or charging capacitor can not be neglected in determining the wave shape. Therefore, the wave shaping circuit neglecting thyratron tube drop is shown in Fig. VI-2

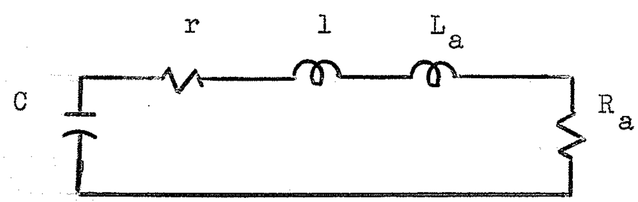

$$e = E(\epsilon^{-at} - \epsilon^{-bt})$$

Fig. VI-2 Wave Shaping Circuit

where r = resistance in leads and capacitor
l = inductance in leads and capacitor
L_a = added inductance
R_a = added resistance

The values of 'r' and 'l' for the three capacitor bank connections are

TABLE VI-1 VALUES OF 'r' AND 'l' FOR THE THREE CAPACITOR BANKS

C uf.	r ohms	l uhenries
35	.25	2.0
10	.30	1.0
.5	.15	.5

The resistances and inductances were measured at 500KC using a GR Model 916 A Radio Frequency Bridge. The measurements were made directly at the external output terminals of the transient visualizer. Therefore, all inductance and resistance in the connecting leads and capacitors was taken into account. During these measurements the discharge thyratron was by-passed by a short length of wire. It is estimated that 'r' is measured at 500 KC to an accuracy of 4%, and 'l' to 6%.

Since capacitance is approximately constant for all frequencies the charging capacitors were measured to a 3% accuracy at 10 KC with a GR 650 Impedance Bridge.

In the above analyses the effect of the test speciman on the wave shape was neglected. In the impulse testing of transformer and machine windings, the capacitance introduced by the test speciman alters the applied wave shape. In the transient visualizer the charging capacitance is large relative to the speciman capacitance and the applied wave shape was altered very slightly. However, in large impulse generators the charging capacitance is usually not large and the wave shaping circuit shown in Fig. VI.1, page 37, may be unsuitable.

CHAPTER VII

POWER REQUIREMENTS AND ASSEMBLY

VII-1. A-C AND D-C POWER REQUIREMENTS

The a-c power circuit is fused as follows: a-c input - 20 amps, variac - 15 amps, d-c power supply - 3 amps, trigger circuit - 2 amps. The total a-c power requirements are 110 volts, 12 amps.

The d-c power requirements are 225 volts - 100 milliamps, 350 volts - 20 milliamps, with no regulation necessary. The filament requirements are 6.3 volts - 6 amps.

A standard power supply was designed and the circuit diagram is shown in Fig. VII-2, page 42. In the d-c supply a Hammond power transformer was selected having the following ratings:

Primary volts = 115

Secondary volts = 450 - 0 - 450

D-C milliamps = 200

Filament = 6.3V., 6.0a. ct

VII-2 ASSEMBLY

The transient visualizer circuits were enclosed in a cabinet 36" x 24" x 54". The supports and braces were constructed of angle iron and the joints were welded together. The sides of the cabinet consisted of wire mesh for cooling purposes and the front and rear of no. 20 gauge steel plate. For appearance the corners were covered with aluminum molding.

The d-c power supply and thyratron trigger circuit chassis were situated on the front of the cabinet, and are easily accessible for servicing. Other controls situated on the front panel are: main a-c power switch, external synchronizing and beam trigger output terminals, peak reading voltmeter and switch.

At the rear of the cabinet the following controls and terminals are present: external transformer input, output terminals, external output for peak voltmeter, two plug board panels with plug boards.

The operating controls were designed so that there is no need to proceed to the rear of the cabinet once the visualizer is in operation. For detailed operating instructions refer to Appendix C.

Photographs of the inside of the cabinet are shown on page 43, and of the cabinet and trigger chassis on page 44.

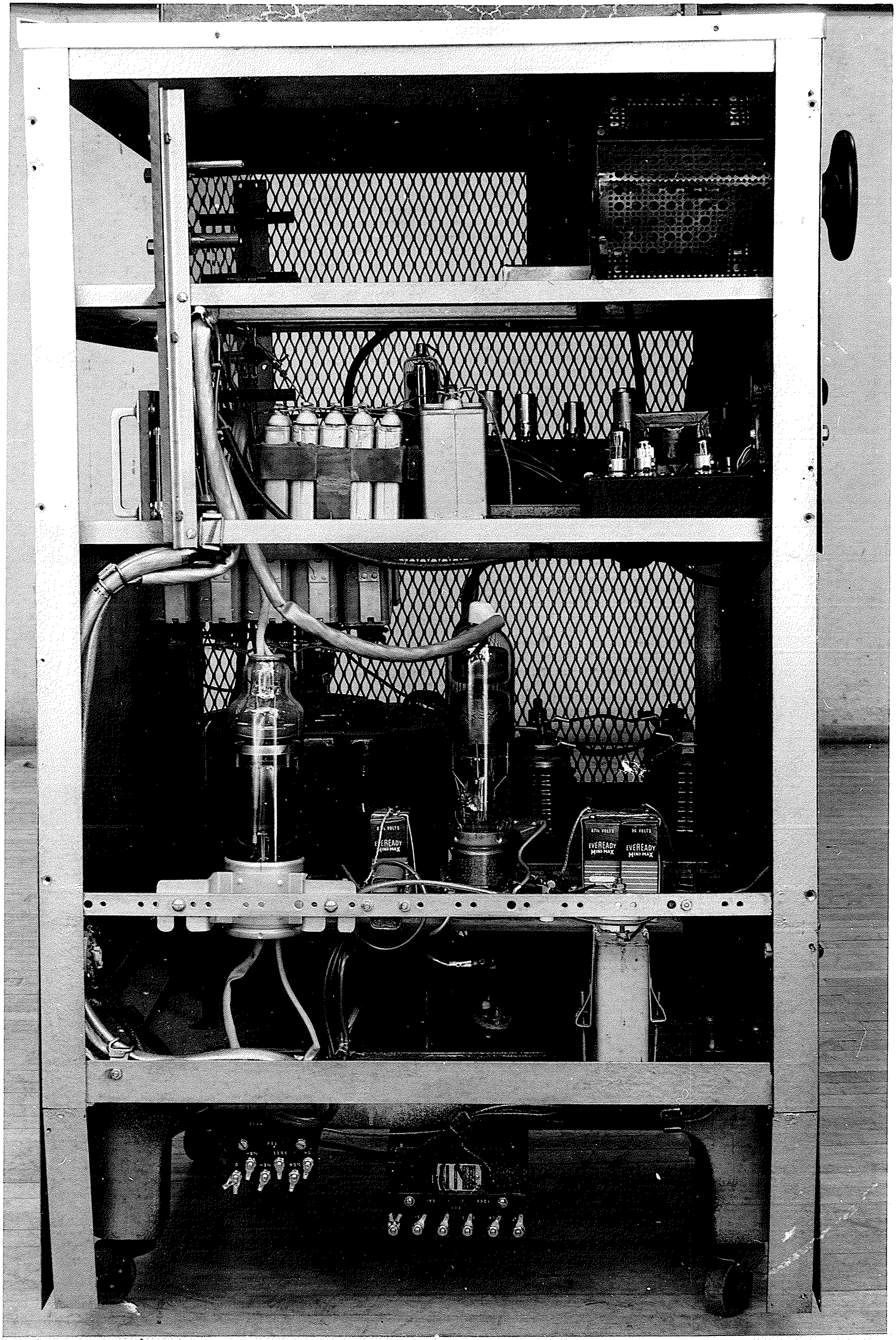
EVEREADY MINI MAX
EVEREADY MINI MAX
EVEREADY MINI MAX

POWER SUPPLY

FIG. VII-2

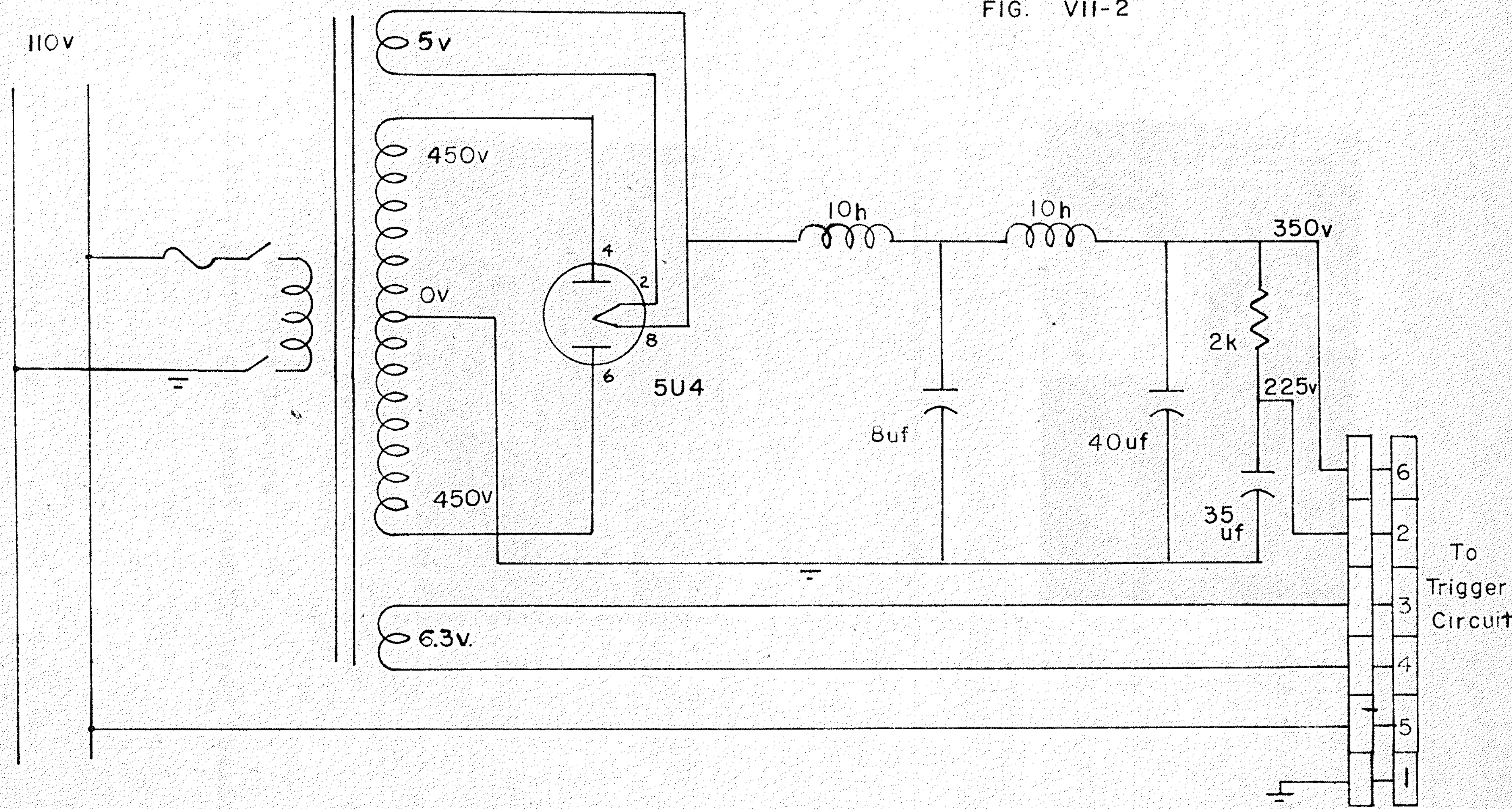

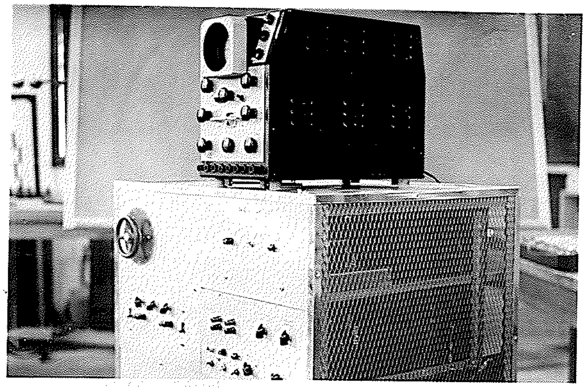

Transient Visualizer Cabinet

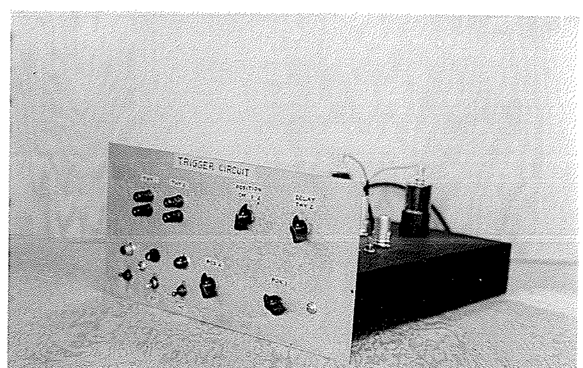

Trigger Chassis

Fig. VII Photographs of Cabinet and Trigger Chassis

PART B

UTILIZATION OF TRANSIENT VISUALIZER

CHAPTER VIII

TRANSIENTS FROM A CAPACITOR DISCHARGE

The transient visualizer in conjunction with an oscilloscope can display a transient voltage or current resulting from a capacitor discharge. Consider the discharge of a capacitor C_1 into an external circuit R_1, C_2, and R_2 as shown in Fig. VIII-1.

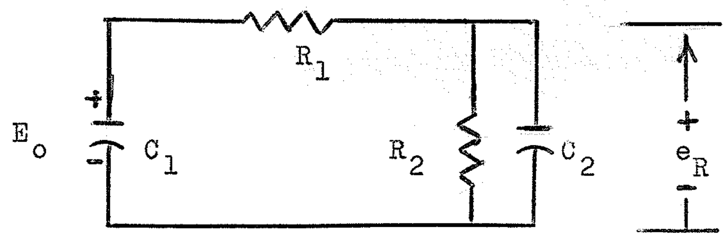

Fig. VIII-1 Resistance Capacitance Discharge Circuit

The output voltage e_R is given by, (Sur 1)

$$e_R = \frac{E_o}{2R_1C_2q}\left[\epsilon^{-(p-q)t} - \epsilon^{-(p+q)t}\right]$$

$$\text{where} \quad p = \frac{R_1C_1 + R_2(C_1+C_2)}{2R_1R_2C_1C_2}$$

$$q = \sqrt{p^2 - 1/R_1R_2C_1C_2}$$

In order to check the operation of the visualizer, the voltage e_R is calculated and compared with the results obtained by an oscilloscope.

Let C_1 = .5 uf

C_2 = 4.0 uf

R_1 = 2900 ohms

R_2 = 1500 ohms

E_o = 270 volts

Then $p = 471$

$q = 326$

and $e_R = 35.7\ (\epsilon^{-145t} - \epsilon^{-797t})$ volts

In Table VIII.1 the voltage e_R is calculated from time $t = 0$ to $t = 20$ milliseconds.

TABLE VIII.1

CALCULATION OF OUTPUT VOLTAGE e_R FOR TIME 't'

t millisec	e_R volts
0	0
.5	9.2
1.0	14.8
1.5	17.9
2.0	19.4
2.5	19.9
3.0	19.8
3.5	19.1
4.0	18.5
5.0	16.6
6.0	14.6
7.0	12.8
8.0	11.0
9.0	9.6
10.0	8.4
12.0	5.9
14.0	4.7
16.0	3.5
20.0	2.7

Table VIII.1 is plotted in Fig. VIII-3, page 48, and the oscillogram results are illustrated in Fig. VIII-2, page 47. Because of the incorrect focusing of the camera, a thick oscillographic trace was obtained on the photograph. Various voltages at the mid point of this trace were plotted against time in Fig. VIII - 3.

Close agreement is found between the calculated and oscillogram wave shapes. The maximum voltage was measured as 20 volts on the oscilloscope and the calculated value was 19.8 volts. The calculation of the above voltage was not too difficult but in a circuit involving parallel paths of inductance and capacitance the derivation and calculation of a voltage or current is very difficult. However, with the use of the visualizer a transient voltage or current can be displayed directly on the screen of an oscilloscope.

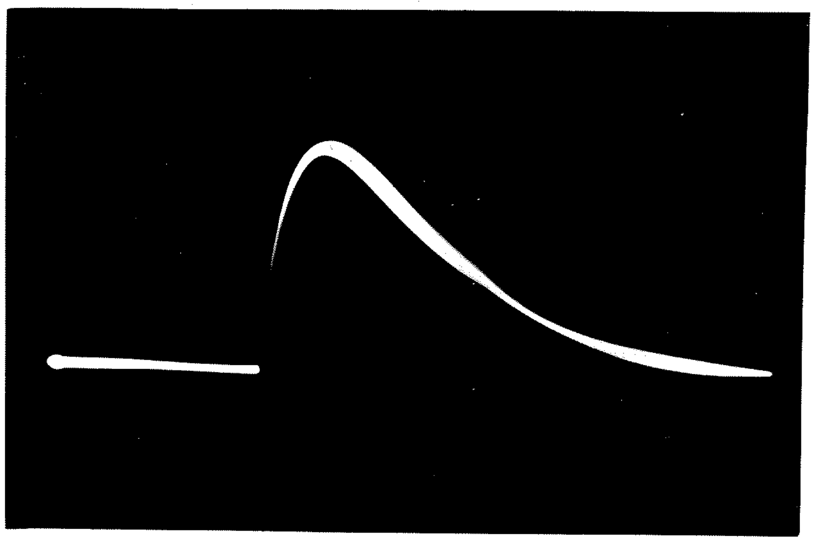

Fig. VIII-2 Oscillogram of Transient Voltage
Vert. Scale 16.7 volts/in. Hor. Scale 8 millisec/in.

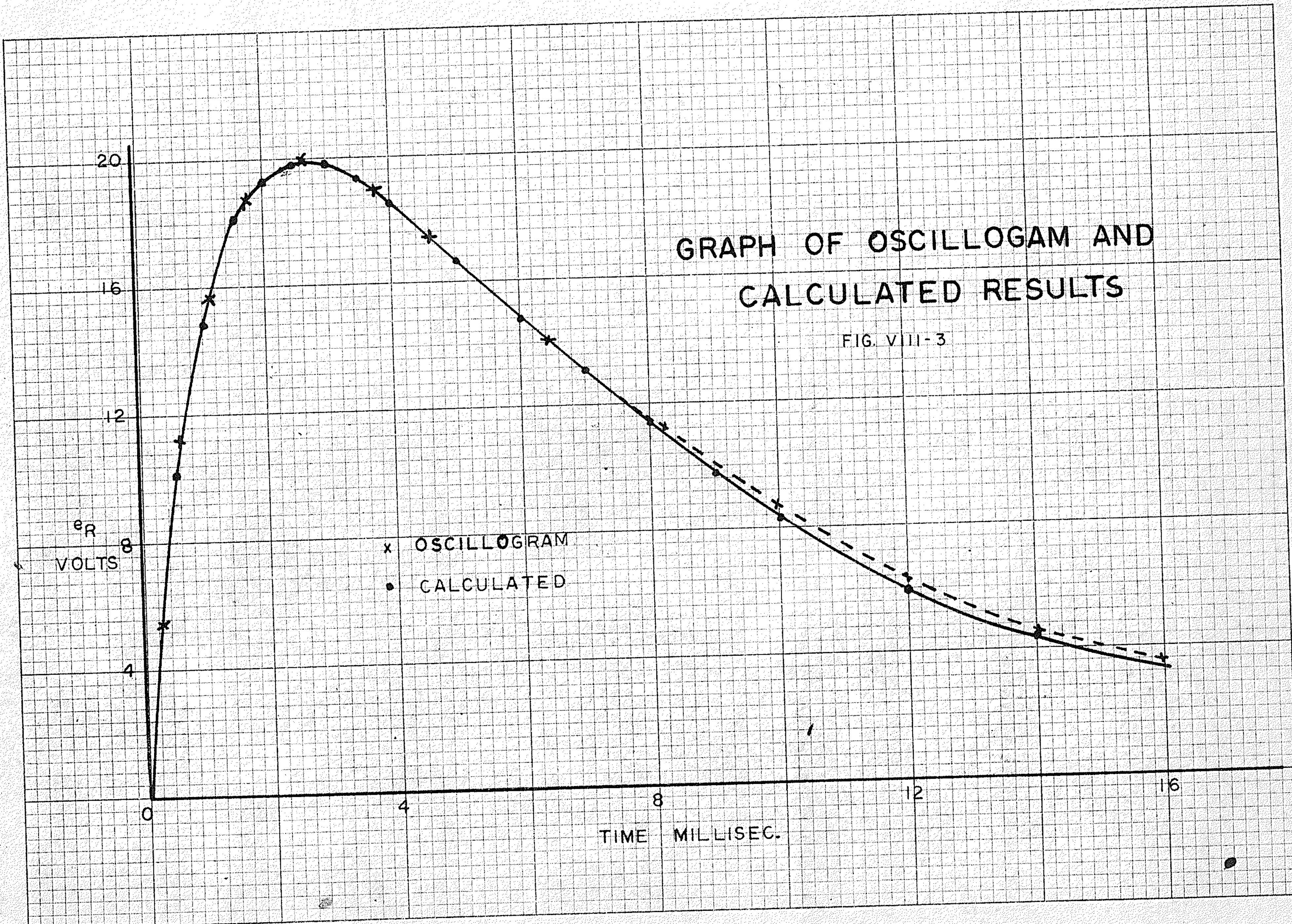

GRAPH OF OSCILLOGAM AND CALCULATED RESULTS

FIG. VIII-3

CHAPTER IX

TESTING OF ELECTRIC WINDINGS

Investigation into disturbances in high tension networks show that short over voltages created by atmospheric discharges, surge phenomena, etc., have an essentially different behaviour compared with high direct or alternating voltages. Therefore, it is desirable to test transformer and electric machinery windings with impulse voltages. Such tests yield valuable data on the electrical materials, leading to the application of materials and construction methods more resistant to over voltages.

IX-1 TRANSFORMER WINDING

A transformer is a very complicated network of resistances, self and mutual inductances, and stray capacitances. At 60 cycles, many of these components are too small to be significant, but they are very important when an impulse wave is applied to the winding. A few of the components in a single-phase transformer are shown in Fig. IX-1.

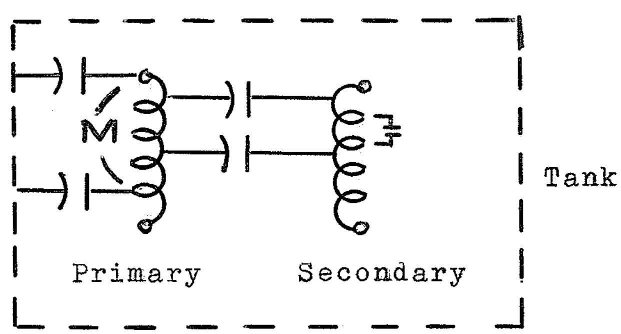

Fig. IX-1 High Frequency Equivalent Circuit of Transformer

When an impulse wave is applied to one end of a transformer it travels along the winding exciting the small oscillatory circuits composed of the inductances in the winding and their associated stray capacitances. These oscillatory circuits alter the impulse wave shape as it travels through the winding. These effects can be demonstrated on a transformer with tap-off points along the winding by the transient visualizer. The standard $1\frac{1}{2}$ x 40 impulse wave is applied directly across the winding (Fig. IX-1a) and the voltage to ground at various tap-off points is measured on a oscilloscope. Fig. IX-2 page 51, shows the voltage waves at various tap-off points. This information can be used for determining the voltage between various coils and this permits the placement of insulation where it is needed most.

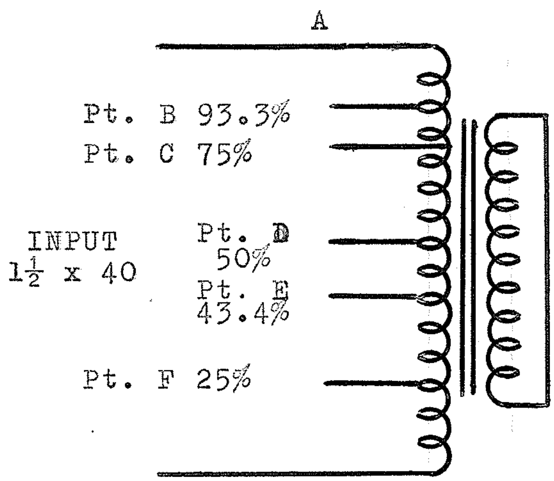

Fig. IX-1a Tap-off Points in a Transformer Winding

IX-2 ELECTRIC MACHINE WINDINGS

In an electric machine winding (a-c motor or generator) the capacitance and inductance elements are well distributed as to physical position, and therefore, have very low over-all capacitive or inductive coupling. This is opposite to the transformer where over-all coupling is high. The distribution of capacitance and inductance is not uniform, but tends to be lumped by coils and pole groups. Therefore, the impulse wave will take on the characteristics of a traveling wave similiar to an artificial transmission line. The electrical length of a motor winding is much greater than the actual length, or stated differently, the velocity of propagation is low. Thus, there is sufficient time lag in the movement of the wave for a large voltage to exist between turns where the rise time of the impulse wave is very rapid. With the use of the transient visualizer these high stress regions can be located and this permits the placement of insulation where it is needed most. The traveling-waves can be demonstrated using a machine winding with tap-off points along one leg of a three phase winding as shown in Fig. IX-3.

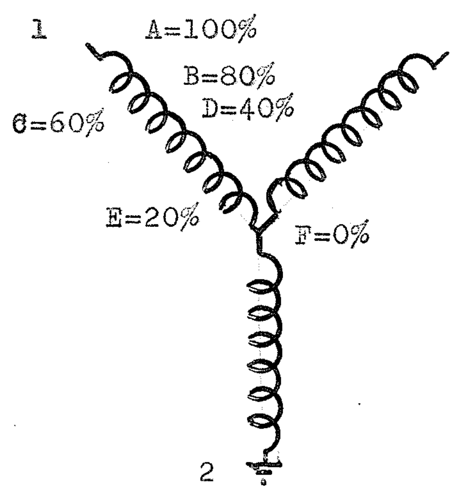

Fig. IX-3 Tap-off Points in a Machine Winding

A $1\frac{1}{2}$ x 40 impulse wave of positive polarity was applied across terminals 1 and 2. Fig. IX-4, page 53, illustrates the voltage wave shapes measured with respect to ground at the various tap points. At first there is a decrease in the voltage amplitude, then it increases due to the reflected wave, reaching a maximum value 30% above that of the applied wave. The oscillograms show the voltage

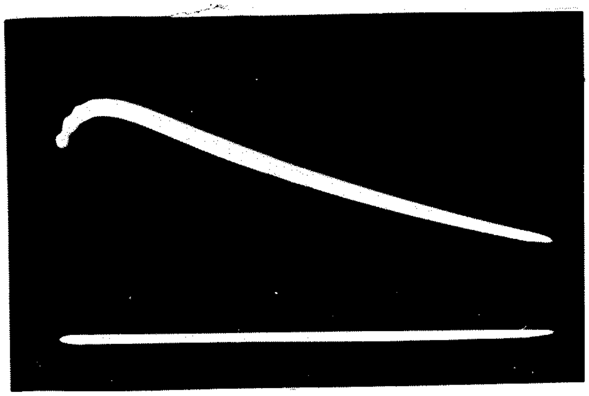

Pt. A, Vert. Scale 400/in.

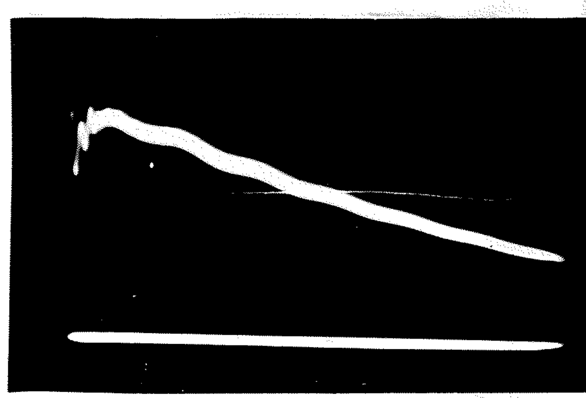

Pt. B, Vert. Scale 400/in.

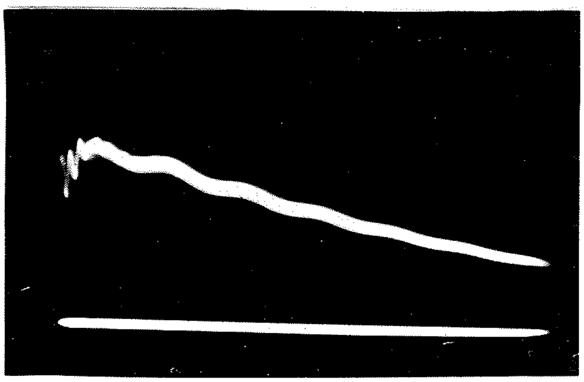

Pt. C, Vert. Scale 400/in.

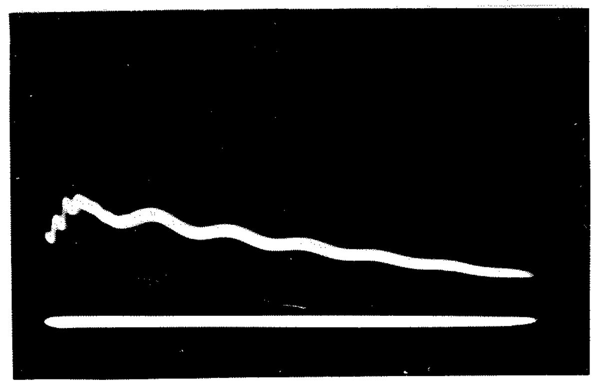

Pt. D, Vert. Scale 400/in.

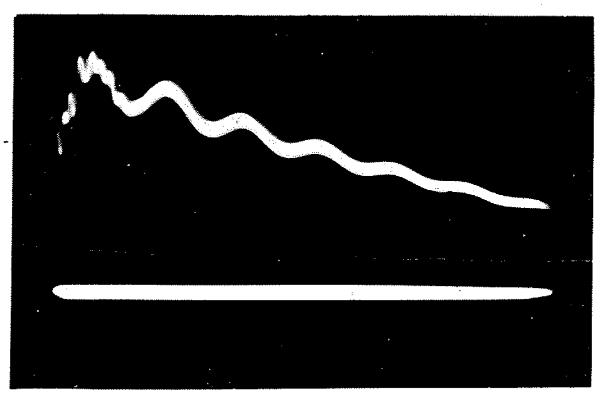

Pt. E, Vert. Scale 200/in.

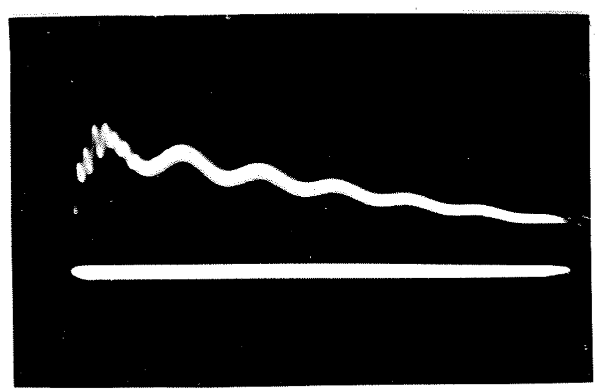

Pt. F, Vert. Scale 200/in

Fig. IX-2, Surge Distribution in Transformer

Hor. Scale 20us/in

variations in a machine winding under conditions of applied impulses, such as are obtainable with switching, lightning, or other circuit variations.

IX-3 PRODUCTION TESTING OF ELECTRIC MOTORS

The speed and accuracy of the transient visualizer makes it invaluable as a production tester on mass-produced three-phase and single-phase motors. The visualizer generates pulses in a periodic manner and these are applied alternately using a synchronous switch to two machine windings as shown in Fig. IX-5, page 54. An oscilloscope is connected from phase 3 to ground.

The synchronous switch consists of a Potter and Brumfield, power type DPDT relay (No. PR11AL8) synchronized to the 60 cycle supply. This is accomplished by converting the 60 cycle sine wave into a square wave with the same period and phase. Then, the square wave is differentiated and the positive pulses are applied to a bistable multivibrator that operates the relay. Thus, the relay switches every cycle and alternate impulses are applied between terminals 1 and 2 in Fig. IX-5, page 54. If the two windings in question are identical the two voltage waves will be identical and the patterns on the screen of the oscilloscope will merge and if the two windings are different, two waveforms will be present on the screen of the oscilloscope. The oscilloscope can be connected to any point on the third winding but experience has shown connection to terminal 3 is more sensitive to winding defects.

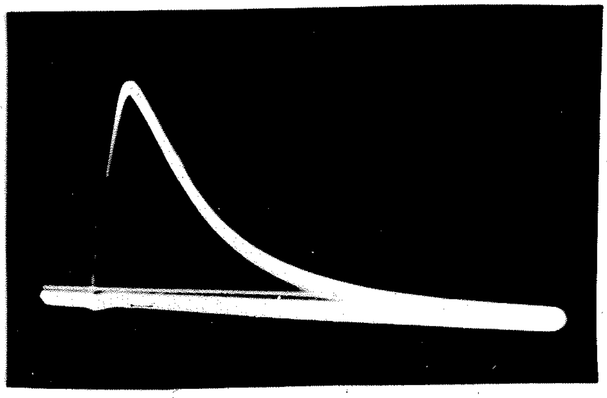

Pt. A.

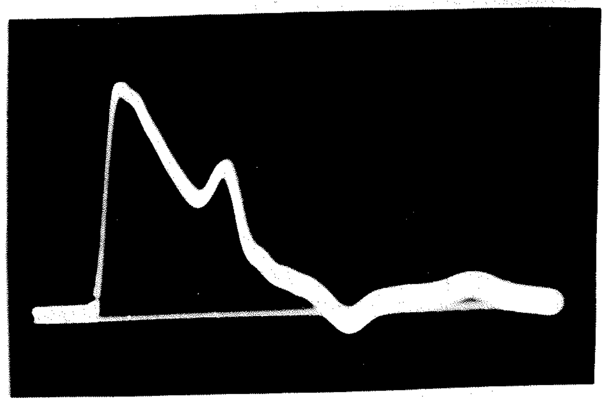

Pt. B.

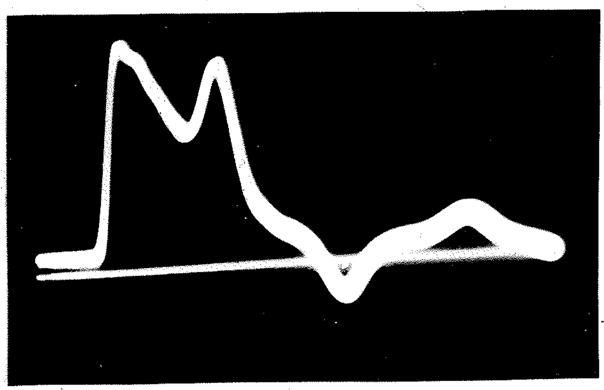

Pt. C.

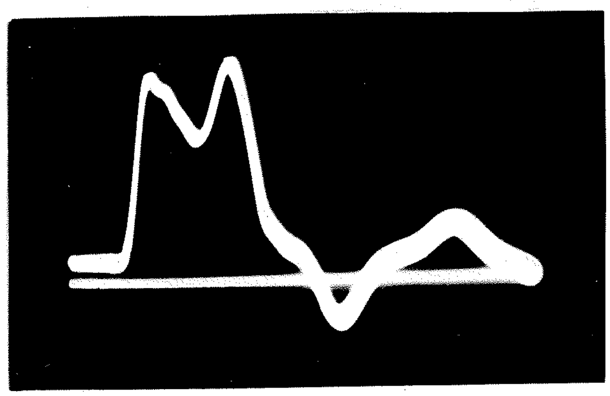

Pt. D.

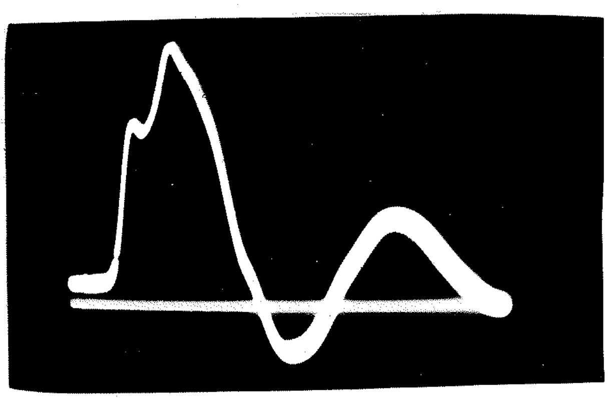

Pt. E.

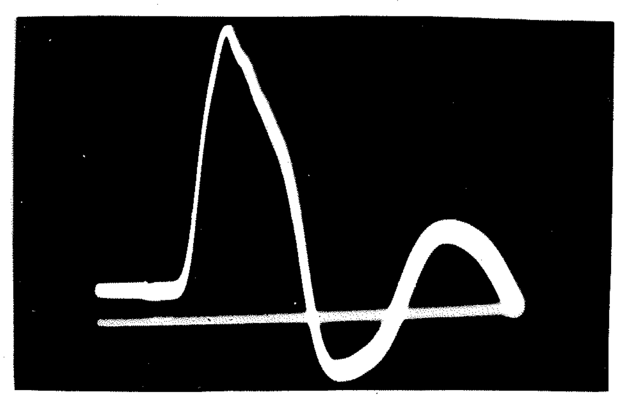

Pt. F.

Fig. III-4, Wave Propagation in Machine Winding

Scales: Vert. 200 v/in., Hor. 40 μs/in.

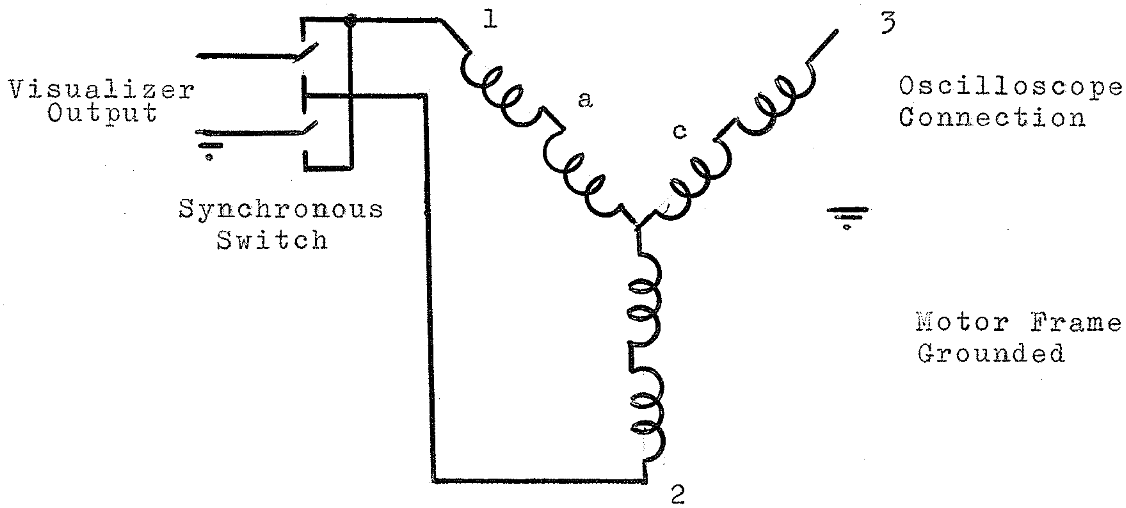

Fig. IX-5 Test Circuit for Determining Faults

Fig. IX-6, page 55, shows oscillograms of winding failures and Table IX.1 indicates the location of the fault.

TABLE IX.1 LOCATION OF FAULTS

OSCILLOGRAM	FAULT LOCATION
1	none
2	1-a shorted
3	pt. 'a' 10 K to ground
4	3-c shorted
5	pt. 2 grounded

Since the winding is symmetrical and no faults are present, a single wave is shown in oscillogram 1. If the symmetry is disturbed by a shorted coil or ground connection, two waves will be displayed on the screen. The effect of a shorted coil is shown in oscillogram 2, and a short to ground through 10K ohms is shown in oscillogram 3. This resistance was used to represent leakage due to poor insulation. In oscillogram 4 there is only one wave displayed showing symmetry in the windings being pulsed. However,

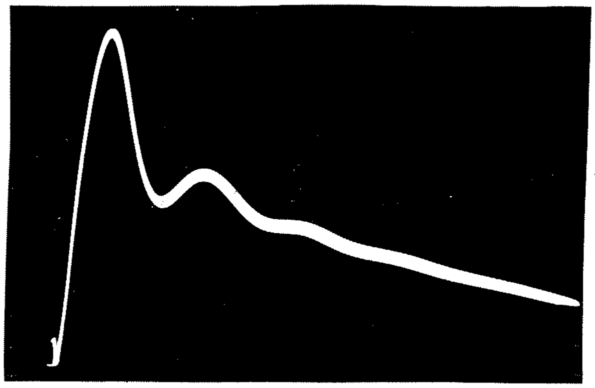

(1)

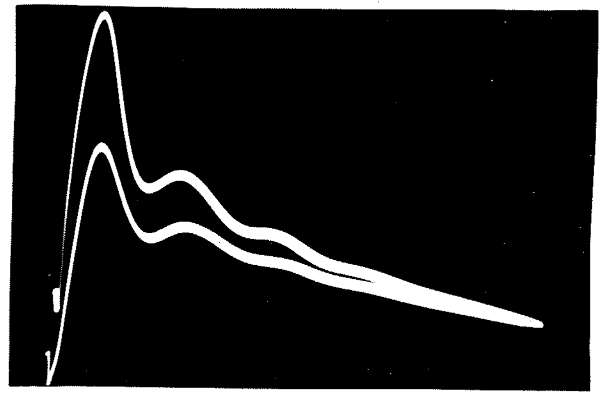

(2)

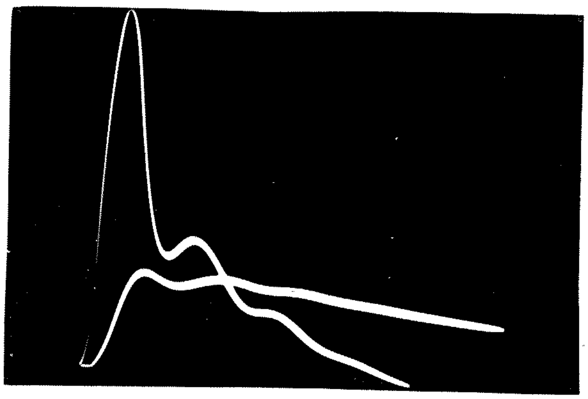

(3)

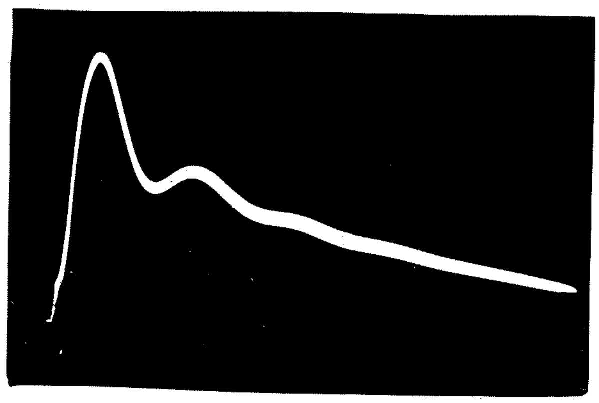

(4)

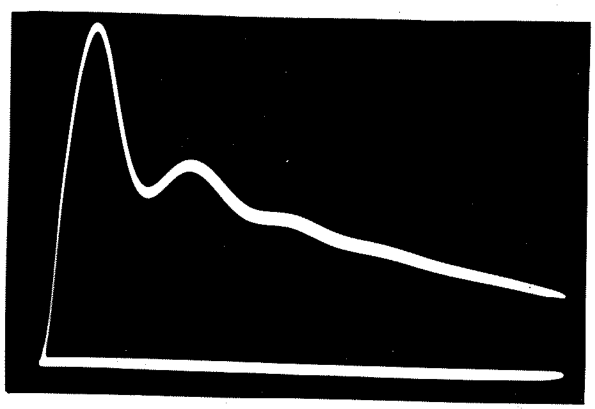

(5)

Fig. [illegible]-5. Oscillograms of winding failures this wave is smaller in magnitude than the waveform in oscillogram 1, indicating a fault in the winding where the oscilloscope is connected. In mass production testing of identical machines this fault would be easily recognized. Oscillogram 5 indicates a short to ground in the main input terminals to the motor. When the impulse wave is applied to terminal 2, the visualizer output is shorted causing a horizontal line on the oscillogram. When the impulse is applied to terminal 1, a waveform is obtained similiar to that in oscillogram 1. Therefore, the relative shapes and amplitudes of the waveforms obtained by the visualizer can be used to indicate the nature of the defect.

In testing single phase motors a standard winding that has been tested thoroughly can be used as a check against identical production units. The oscilloscope is connected from point A to ground as demonstrated in Fig. IX-7. The operator passes those motors which coincide with the standard and rejects those motors which display a pattern which is different.

The above test procedure is very fast, which enables it to be used in a high-speed production line. The main disadvantage is the difficulty in classifying the fault, and therefore, auxilary equipment is required for fault location.

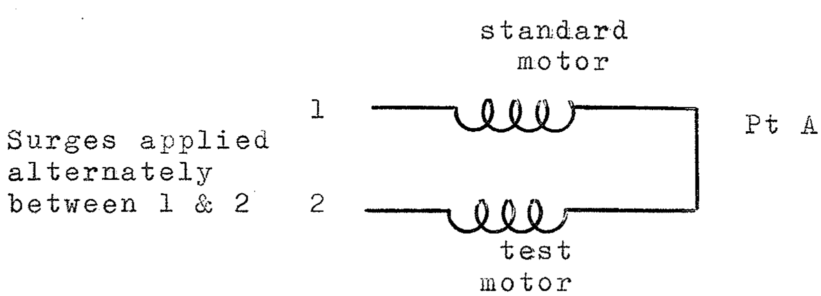

Fig. IX-7 Testing of Single-Phase Motors

CHAPTER X

COAXIAL CABLE TERMINATION OF A VOLTAGE DIVIDER

In high voltage impulse testing the peak voltage applied to a circuit is of the utmost importance. The cathode ray oscilloscope is an excellent instrument for recording peak voltages, and also, it shows the effect of the external circuit on the impulse wave. However, a suitable voltage divider must be designed for reducing the impulse voltage to proportions which will permit its application to the oscilloscope deflection plates.

A voltage divider should accurately reproduce across the deflection plates of the oscilloscope the impulse wave applied to the test piece regardless of the wave shape. One of the common and widely used types of dividers is the resistance cable divider. The arrangement of the resistance cable divider is shown in Fig. X-1.

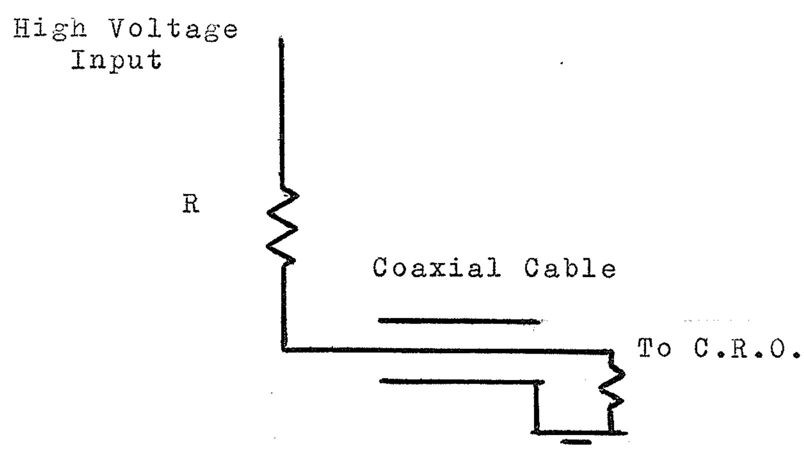

Fig. X-1 High Voltage Divider

The exact impedance termination at the end of the cable is very important and must equal the surge impedance of the cable. If the impedance is decreased below the surge impedance of the cable, reflections will occur in the cable which tend to increase the magnitude of the applied wave, and also decrease the time to reach crest. If the impedance is increased above the surge impedance, the output wave is decreased in magnitude, and time to reach the crest is increased. With a superimposed oscillation on an impulse wave, a small mismatch will cause a large error in the peak voltage.

When a complex waveform is applied to a coaxial cable, the very low frequency components of the wave encounter a different characteristic impedance than the very high frequency components. The characteristic or surge impedance is given by

$$Z = \sqrt{\frac{r + jwl}{g + jwc}} \qquad \text{X.1}$$

As the frequency increases, the resistance 'r' increases and the inductance 'l' decreases because of skin effect. Also the conductance 'g' increases slightly due to an increase of dielectric loss with frequency. Thus, for each frequency component of a complex waveform there is a different surge impedance, and the calculation of an 'optimum' matching impedance is extremely difficult.

Because the surge impedance is highly resistive the cable can be terminated in a resistance. By using a variable resistor the correct termination can be determined by the application of a highly oscillatory wave and a smooth wave with the same peak voltage. Now, by varying the terminating resistance a value will be found that will give the same deflection for both waves. To perform such a test in a high voltage laboratory, spheres are required to keep the peak voltages equal, and photographs to check the deflection of each wave on the oscilloscope. Therefore, numerous tests would be performed before an equal deflection was obtained for both waves.

With the use of the transient visualizer the above calibration can be performed at very low voltages. The speed and accuracy of the instrument makes it invaluable in determining the correct resistance termination.

A model resistance cable divider was constructed but it is not suitable for high voltage testing due to the low wattage rating of the resistors employed. However, tests on such a divider would simulate tests on an actual high voltage divider. The divider consists of 33K ohms of resistance at the impulse generator end. Approximately 100 feet of Amphenol RG - 58A/U coaxial cable with a nominal impedance of 50 ohms was used to connect the divider to the oscilloscope.

Fig. X-2, page 60, illustrates the effect on the magnitude of a waveform when the terminating resistance is varied. The cable was found to be matched when terminated in 53 ohms. This value was obtained by applying from the visualizer a smooth and then an oscillatory wave of the same voltage to the input of the divider (i.e. method described for high voltage calibration.) However, both wave shapes are at relatively low voltages, and thus, the peak input voltages can be measured by connecting directly to the plates of an oscilloscope.

A highly oscillatory wave was applied to the divider and the peak output voltage (Fig. X-2) was measured for three resistance terminations. The percentage error in the peak voltages due to mismatch is listed in Table X-1.

TABLE X-1 EFFECT OF RESISTANCE TERMINATION

Resistance	Peak Voltages	% Error
48	3.35	5.3
53	3.18	0
58	2.70	15

The above results indicate that a mismatch in the terminating resistance can cause an appreciable error in the measurement of peak voltages. However, with the transient visualizer the correct terminating resistance can be obtained accurately and quickly.

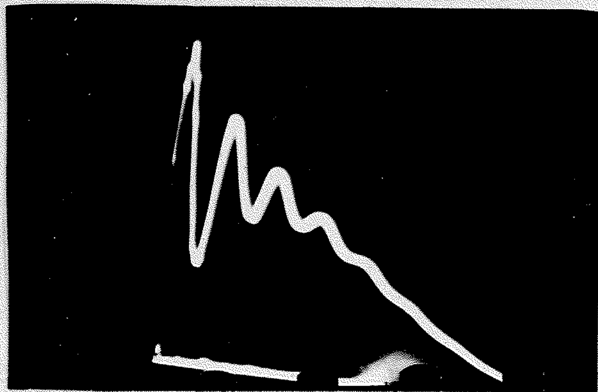

Fig. X-2a, 48 ohms

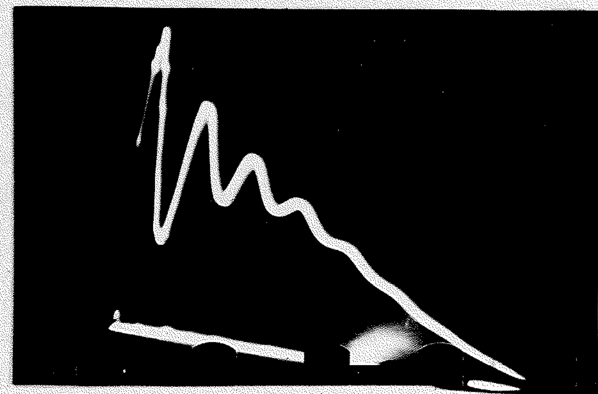

Fig. X-2b, 53 ohms

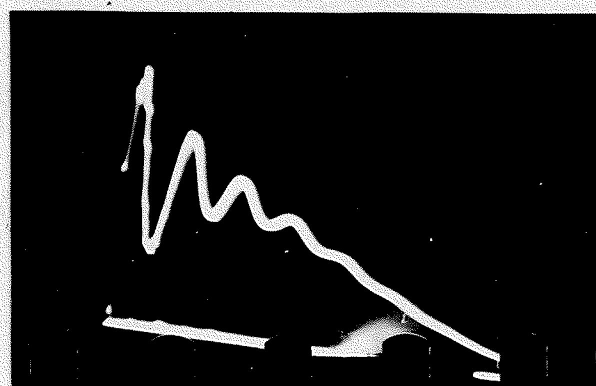

Fig. X-2c, 58 ohms

Fig. X-2, Output wave for resistance terminations

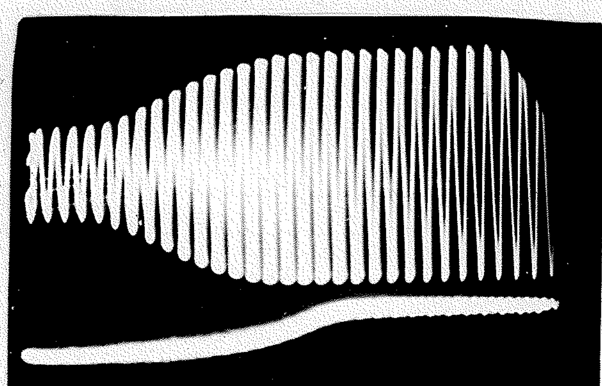

Fig. XI-3a

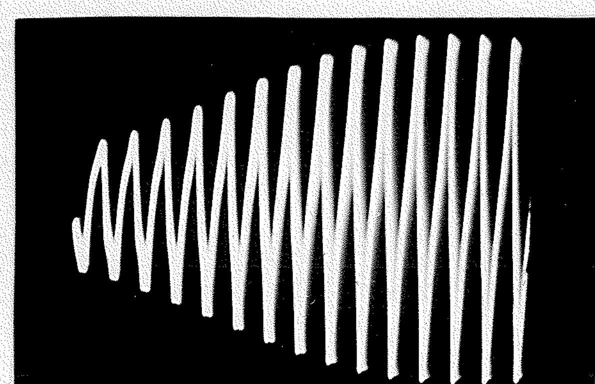

Fig. XI-3b

Magnetic Amplifier Response

CHAPTER XI

MAGNETIC AMPLIFIER

It is very difficult to form an exact equivalent circuit of most electrical apparatus, and more difficult to analyze by mathematical methods the transient response. W. Tishinski* encountered such a problem while investigating the response of the a-c winding of a magnetic amplifier on application of a unit step to the d-c winding. Since a mathematical treatment would be difficult due to the complex equivalent circuit, Tishinski applied a unit step to the d-c winding and photographed the results on an oscilloscope. The circuit used by Tishinski is shown in Fig. XI-1.

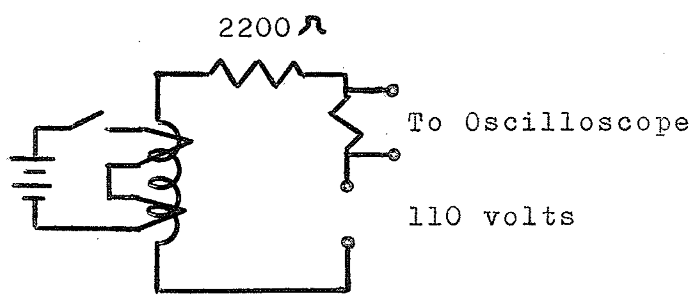

Fig. XI-1 Tishinski's Test Circuit

The auxiliary circuit required to start the sweep (not shown in diagram) before the transient was initiated was very complex. The developing of the film and in some cases the rephotographing of the response was a time consuming task.

However, by the use of the transient visualizer the response is obtained readily. By approximating the unit step by an exponential wave with a very long time constant results were obtained from the transient visualizer that

* Graduate Student, University of Manitoba.

agreed with Tishinski's results. The input to the d-c winding is shown in Fig. XI-2.

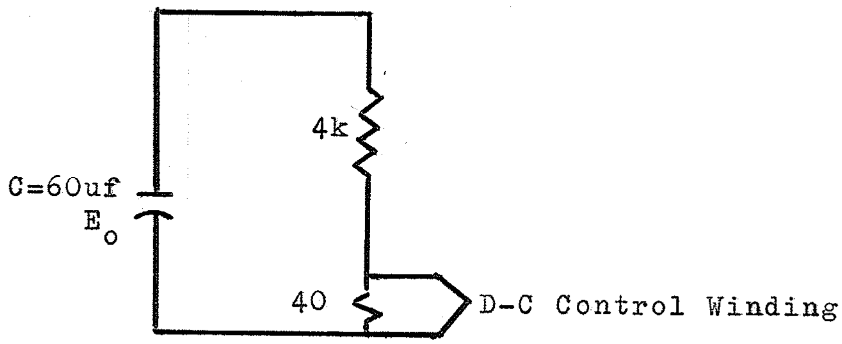

Fig. XI-2 Transient Visualizer Output Circuit

The a-c response obtained by the transient visualizer is shown in Fig. XI-3b, page 60, and Tishinski's results in Fig. XI-3a. By comparing the photographs it is seen that the two results are in very close agreement. The photograph obtained by the visualizer is presented only for comparison purposes. By varying the applied voltage E_o the response can be determined for different input currents. Thus, the transient visualizer is an excellent instrument for displaying long duration transients similiar to those encountered in a magnetic amplifier. The instrument can be an aid in the design of magnetic amplifiers requiring a fast response. Circuit elements can be varied and the effect on the response can be quickly obtained on an oscilloscope.

CHAPTER XII

CONCLUSIONS

The purpose of this thesis was to give a brief description of the design of the transient visualizer and to cite some of the applications for the instrument. The visualizer when used in conjunction with an oscilloscope has proven to be very useful in the determination of winding stresses, magnetic amplifier response, and coaxial cable termination of a potential divider. The facility and certainty of operation, combined with the speed with which results may be obtained are the important features of the transient visualizer in its application in transient analysis.

BIBLIOGRAPHY

BIBLIOGRAPHY

A. BOOKS AND REPORTS

Bew 1. Bewley, L. V., Traveling Waves on Transmission Systems, John Wiley & Sons, Inc., New York, 1951, p. 17.

Dav 1. Davis, Wells L. and Harman R. Weed, Industrial Electronic Engineering, Prentice Hall, Inc., Englewood Cliffs, N. J., 1954.

Gla 1. Glasoe, G., and J. Lebacqz, Pulse Generators, Radiation Laboratory Series, Vol. 5, McGraw-Hill Book Company, Inc., New York, 1948.

Gui 1. Guillemin, E., Synthesis of Passive Networks, John Wiley & Sons, Inc., New York, 1957.

Mar 1. Martin, T., Electronic Circuits, Prentice Hall, Inc., Englewood Cliffs, N. J., 1955, p. 667, 681.

Mil 1. Millman, J., and H. Taub, Pulse and Digital Circuits, McGraw-Hill Book Company, Inc., New York, 1956.

Par 1. Parker, P., Electronics, Edward Arnold Ltd, London, 1950, p. 739.

Sto 1. Storer, J., Passive Network Synthesis, McGraw-Hill Book Company, Inc., New York, 1957. P. 182.

B. SCIENTIFIC PAPERS

Buc 1. Buchanan, L., The Application of Surge Comparison Testing Equipment to Fractional Horsepower A.C. Stator Windings, Trans. AIEE, 1946, 65 p. 1356

Fou 1. Foust, C., and Rohats, M. Insulation Testing of Electric Windings, Trans. AIEE, 1943, 62, p. 203.

Hag 1. Hagenguth, J., Progress in Impulse Testing of Transformers, Trans. AIEE, 1944, 63, p. 999.

Mos 1. Moses G. and Harter, E., Winding-Fault Detection and Location by Surge Comparison Testing, Trans. AIEE, 1945, 64, p. 499.

Roh 1. Rohats, N., The Oscillograph Electric Transient Analyzer, General Electric Review, 1936, 39, p. 146.

Str 1. Strain, R., Some Aspects of Surge Comparison Testing of Fractional-Horsepower Motors, Trans. AIEE, 1957, 75, Pt III, p. 917.

Sur 1. Surge Phenomena, Seven Years Research for the Central Electricity Board, p. 154.

Wil 1. Wilkinson, K., Recurrent-Surge Oscillographs and their Application to Short-Time Transient Phenomena, JIEE, 1938, 83, p. 663.

APPENDICES

APPENDIX A

In the case of switching circuits the problem of analytical analysis can be greatly simplified by linear approximation of the tube characteristics. Consider the grid and plate characteristics of a vacuum tube as shown in Fig. A-1.

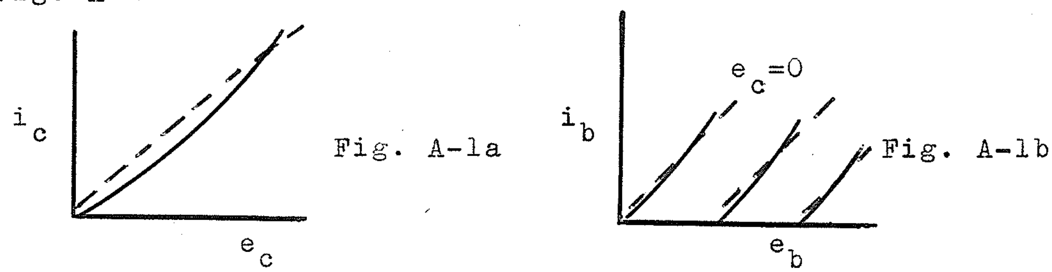

Fig. A-1 Grid and Plate Characteristics

The curves in Fig. A-1 can be represented by straight lines as indicated on the characteristics. Then, Fig. A-1a can be represented by the following circuit.

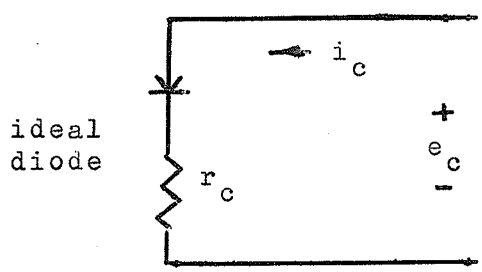

Fig. A-2 Circuit Representation of Grid Characteristic

In Fig. A-1b, assume that the curve for $e_c=0$ passes through the origin. Then, for $e_c=0$, the plate circuit can be represented by an ideal diode inserted in series with a resistance r_p. For other values of e_c the characteristic is shifted to the right or left depending on the polarity of e_c. This shift can be accounted for by adding a generator in series with r_p. Thus, the plate circuit can be represented by the diagram in Fig. A-3.

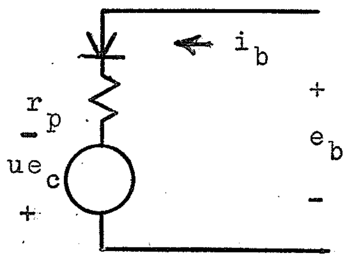

Fig. A-3 Circuit Representation of Plate Characteristic

If the curve for $e_c = 0$ does not pass through the origin a voltage E must be added to account for this shift. In triodes the voltage E is usually small and therefore can be neglected.

The combined grid and plate circuit diagram is shown in Fig. A-4.

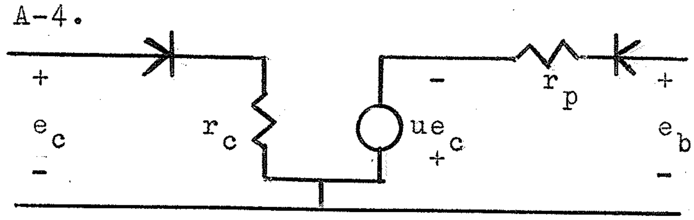

Fig. A-4 Combined Grid and Plate Circuits

The period of the multivibrator circuit shown in Fig. A-5 will be calculated in terms of the circuit constants. In the analysis the triode is replaced by its equivalent circuit obtained from linear approximations of the tube characteristics. The method of analysis is similiar to that performed by Martin. (Mar 1)

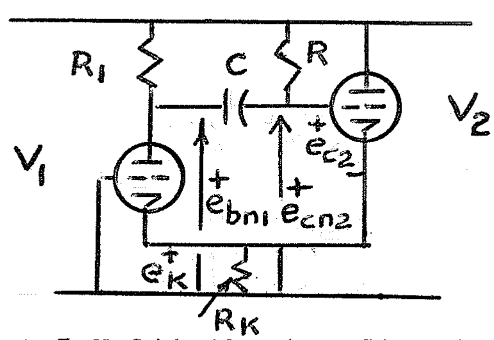

Fig. A-5 Multivibrator Circuit

In the normal state V_1 is cut off and V_2 is conducting. The equivalent circuit of the V_1 amplifier is shown in Fig. A-6.

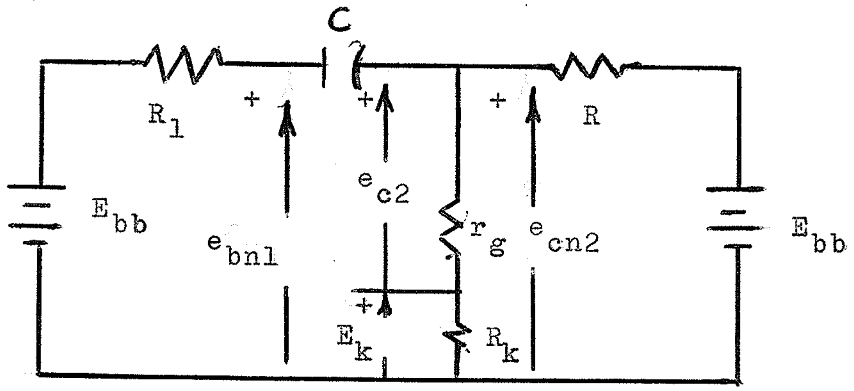

Fig. A-6 Equivalent Circuit When V_2 Conducts

Since no transients are present, no current flows through C and R_1.

Thus $I_g = \frac{E_{bb}-E_k}{R + r_g}$

and $e_{c2} = I_g r_g = \frac{E_{bb}-E_k}{R + r_g} r_g$

Knowing e_{c2} and the d-c load line the quiescent plate current can be found.

$$\text{Then } e_{cn2} = e_{c2} + I_{b2}R_k \doteq 0 + E_k \doteq E_k \qquad \text{A.1}$$

$$\text{Also } e_{bn1} = E_{bb}$$

The voltage across the capacitor C is

$$V_c = e_{bn1} - e_{cn2} = E_{bb} - E_k \qquad \text{A.2}$$

When a negative pulse is applied at time t=0, V_2 stops conducting, the voltage across R_k drops to zero and V_1 starts conducting. Consider the equivalent circuit of V_1 for t=0+ as shown in Fig. A-7 page 69.

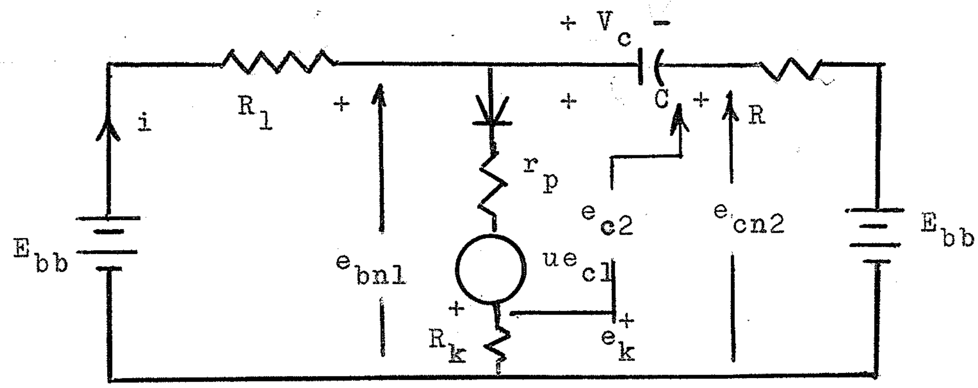

Fig. A-7 Equivalent Circuit When V_1 Conducts

Now $e_{c1} = -e_k$

and $ue_{c1} = -ui_{b1}R_k$

Fig. A-7 can be replaced by Fig. A-8

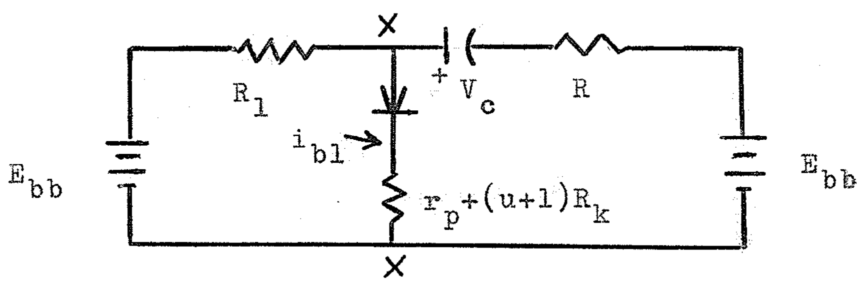

Fig. A-8 Revised Equivalent Circuit

Replace the circuit to the left of the points X-X by its equivalent Thevenin generator and internal impedance.

$$R_e = \frac{R_1\left[r_p + (u+1)R_k\right]}{R_1+r_p+(u+1)R_k} \qquad \text{and } E_e = E_{bb} - \frac{E_{bb}R_1}{R_1+r_p+(u+1)R_k}$$

Consider the revised equivalent circuit in Fig. A-9.

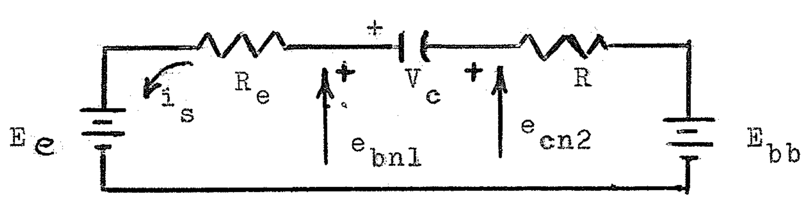

Fig. A-9 Revised Equivalent Circuit

The transient discharge current is

$$i_s = \frac{E_{bb} - E_e + V_c}{R + R_e} \epsilon^{-t/(R+R_e)C} \qquad A.3$$

$$\text{but } E_{bb} - E_e = \frac{E_{bb}R_1}{R_1 + r_p + (u+1)R_k} = A\, E_{bb} \qquad A.4$$

$$\text{where } A = R_1 / \left[R_1 + r_p + (u+1)R_k\right]$$

Substitute equations A.2 and A.4 into equation A.3 and obtain $i_s = \frac{E_{bb}(A + 1) - E_k}{R + R_e} \epsilon^{-wt}$ where $w = 1/(R + R_e)C$

$$\text{Now } e_{bn1} = E_e + i_s R_e$$

$$= E_{bb}(1-A) + \frac{\left[E_{bb}(A+1) - E_k\right]R_e}{R + R_e} \epsilon^{-wt}$$

Since $R \gg R_e$ the transient term is small compared to the steady state term. Therefore, $e_{bn1} = E_{bb}(1-A)$

From Fig A-7 page 69 $i = (E_{bb} - e_{bn1})/R_1 = A\, E_{bb}/R_1$

$$\text{also } e_k = (i_s + i)R_k$$

$$\text{If } i \gg i_s \text{ then } e_k = iR_k = A\, E_{bb}R_k/R_1$$

$$\text{also } e_{cn2} = E_{bb} - i_s R$$

$$= E_{bb} - \frac{\left[E_{bb}(A+1) - E_k\right]R}{R_e + R} \epsilon^{-wt}$$

$$\text{Since } R \gg R_e \qquad e_{cn2} = E_{bb} - \left[E_{bb}(A+1) - E_k\right]\epsilon^{-wt}$$

$$\text{Therefore} \qquad e_{c2} = e_{cn2} - e_k$$

$$= E_{bb} - \left[E_{bb}(A+1) - E_k\right]\epsilon^{-wt} - \frac{AE_{bb}R_k}{R_1} \qquad \text{........A.5}$$

Designate the time self triggering occurs as T. At $t=T$, $e_{c2}=E_{co2}=$ grid cut off voltage. Since the transition times are very short in duration, the period of the multivibrator equals T. The period T can be calculated from equation A.5, page 70.

$$\text{Therefore} \quad T = \frac{1}{w} \ln \frac{E_{bb}(A+1) - E_k}{E_{bb} - E_{co2} - \frac{A\, E_{bb} R_k}{R_1}} \qquad \text{A.6}$$

APPENDIX B

PROOF OF EQUATIONS VI.6 AND VI.7

In the following analysis a fundamental knowledge of network synthesis is required (Gui 1). From equation VI.1 the output voltage is

$$e = e_2(t) = E(\epsilon^{-at} - \epsilon^{-bt})$$

thus
$$e_2(s) = E\left[\frac{1}{s+a} - \frac{1}{s+b}\right]$$

$$= E\left[\frac{b - a}{(s+a)(s+b)}\right] \qquad \text{B.1}$$

Energy is supplied from a capacitor C with an initial charge V_o. This is equivalent to an admittance of value Cs in parallel with a current source CV_o in the complex frequency domain, as illustrated in Fig. B-1.

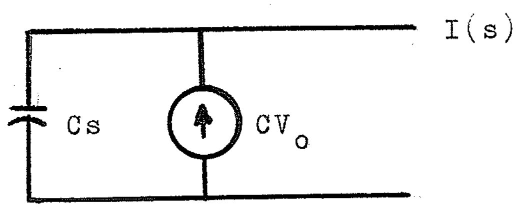

Fig. B-1 Source Representation in 's' Domain

Consider the transfer impedance

$$Z_T(s) = e_2(s)/I(s) \qquad \text{B.2}$$

where $e_2(s)$ and I(s) are represented by the following diagram.

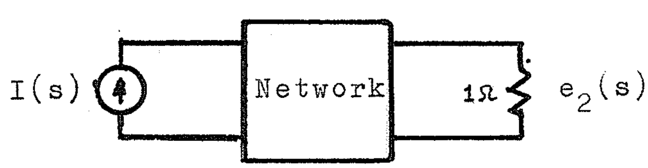

Fig. B-2 Representation of I(s) and $e_2(s)$

Consider only the current source in Fig. B-1 and arrange the network so a capacitance appears across the input. Then, substituting values for I(s) and $e_2(s)$ in equation B.2.

$$Z_T(s) = \frac{E(b-a)}{CV_o}\left[\frac{1}{(s+a)(s+b)}\right]$$

$$= \frac{H}{s^2 + (a+b)s + ab}$$

where $H = \frac{E(b-a)}{CV_o}$

In terms of self and mutual impedances the transfer impedance is given by

$$Z_T(s) = \frac{Z_{12}(s)}{1 + Z_{22}(s)}$$

Since $Z_{22}(s)$ must be a realizable reactance and $Z_{12}(s)$ a "reactance like" function (Sto 1) this leads to the following identifications:

$$Z_{12}(s) = \frac{H}{s(a+b)}$$

$$Z_{22}(s) = \frac{s^2 + ab}{s(a+b)}$$

Now synthesize $Z_{22}(s)$ as a ladder network in such a way that the zeros of $Z_{12}(s)$ are produced. However, $Z_{22}(s)$ has a pole, at infinity, which is not present in $Z_{12}(s)$. Removing this pole the following is obtained.

$$Z_{22}(s) = \frac{s}{a+b} + \frac{ab}{s(a+b)}$$

Let $Z_{22}{}^1(s) = \frac{ab}{s(a+b)}$

Now both $Z_{22}{}^1(s)$ and $Z_{12}(s)$ have a zero at infinity.

Therefore, the final circuit is given in Fig. B-3

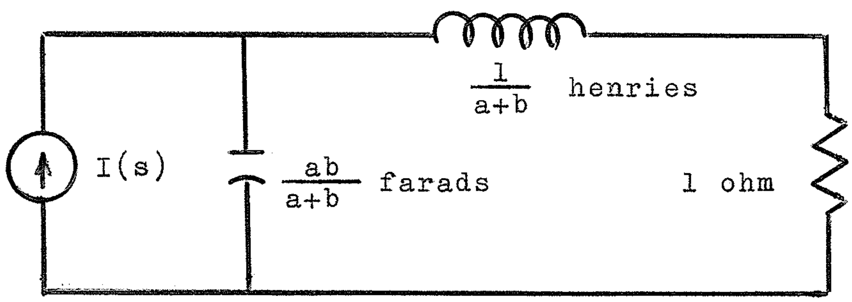

Fig. B-3 Network Synthesizing

$$Z_T(s) = \frac{H}{(s+a)(s+b)}$$

Regardless of the value of H the product RC and LC will always be the same. Since the capacitance is a fixed quantity in the transient visualizer, express R and L in terms of C.

Therefore, $R = \frac{a+b}{Cab}$ ohms B.3

$L = 1/Cab$ henries B.4

if C is in farads.

The effect of the test speciman on the applied wave shape was neglected in the above analyses. If the charging capacitance is relatively large compared to the test speciman capacitance the applied wave shape is only altered slightly. Thus, it is advisable to choose C as large as possible while maintaining the peak current below the maximum permissible value.

APPENDIX C.

OPERATION

The following instructions decide the step by step procedure that is recommended to assure proper operation of the equipment.

1. Before applying power to the cabinet, remove plug boards and check that all switches are off.
2. Proceed to rear of cabinet and make link connection for internal or external transformer.
3. Decide on capacitor bank and make link connection.
4. Turn on main a-c power switch.
5. Check filament and bias voltages for all thyratrons.
6. Select high or low voltage discharge thyratron and replace plug board.
7. Connect wave shaping circuit, load and oscilloscope to output terminals.
8. Replace capacitor plug board.
9. Connect external transformer if required.
10. Proceed to front of cabinet and turn on d-c power supply.
11. Turn on a-c filament supply for trigger circuit and wait ½ minute.
12. Turn on d-c and then a-c power to trigger circuit.
13. Select slow repetition rate and apply charging voltage observing output on oscilloscope. Increase repetition rate making sure transients have sufficient time to decay before next transient occurs.
14. If procedure to the rear of the cabinet is necessary, turn off charging voltage and trigger circuit. Then <u>remove both plug boards</u> and make necessary changes in output circuit.

If the above instructions are followed no harm can occur to individuals or damage to equipment.